# Very Long Baseline Interferometry (VLBI) Lecture I

H. Schuh, L. Plank

1. Introduction:

# *Very Long Baseline Interferometry*

- 1933 (Karl Jansky): 1st measurement of radio signals
- Fast development after WW2 (parabolic antenna)
- Increasing resolution through local inteferometry (100-200 m)
- Local radio interferometry connected by cables
- Atomic clocks (1960ies)
- 1976: Very Long Baseline Interferometry (VLBI)

→ increase the distance (*very long baseline*)

→ no longer connected by cables

*VLBI is interesting for geodesy, because the basic equation of radio interferometry includes besides the **position of the radio source** also the **orientation and length of the baseline vector between the antennas**. Nevertheless, in order to derive from the quite weak and noisy signals geodetic parameters with high precision, a strong cooperation with other disciplines is needed.*

**2. VLBI - basics:**

# Components

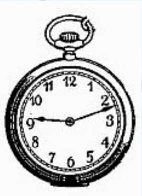

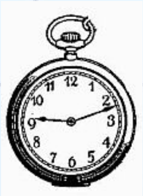

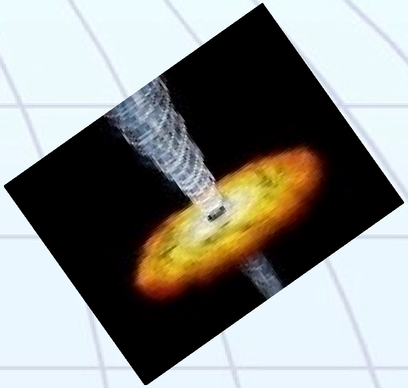

signal (radiation of a quasar)

At least 2 radio telescopes with highly precise atomic clocks

Recording unit (tapes, magnetic discs)

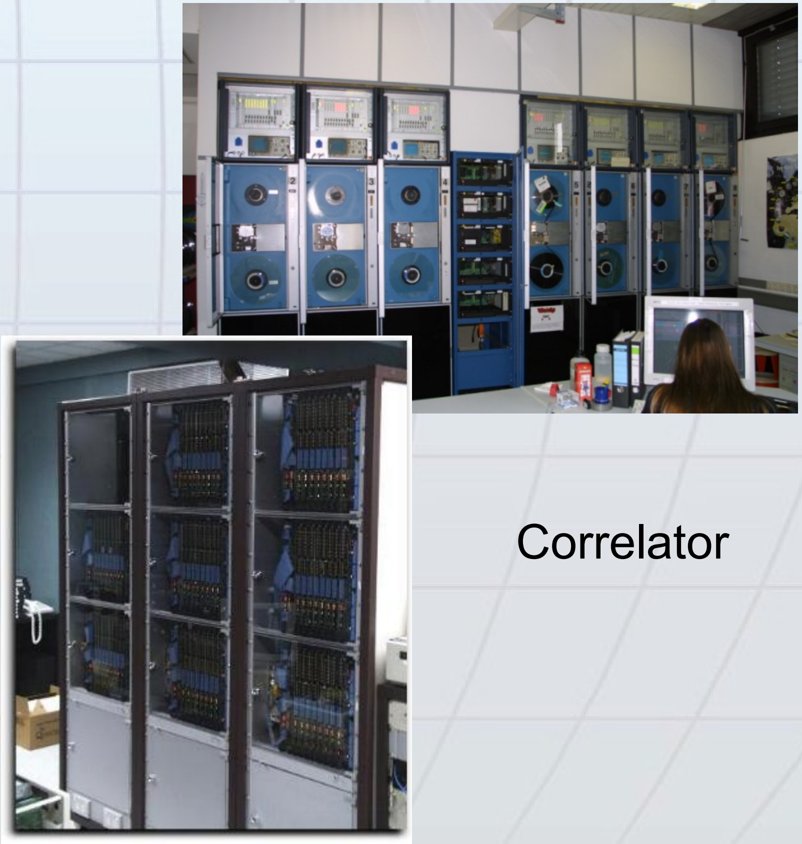

Correlator

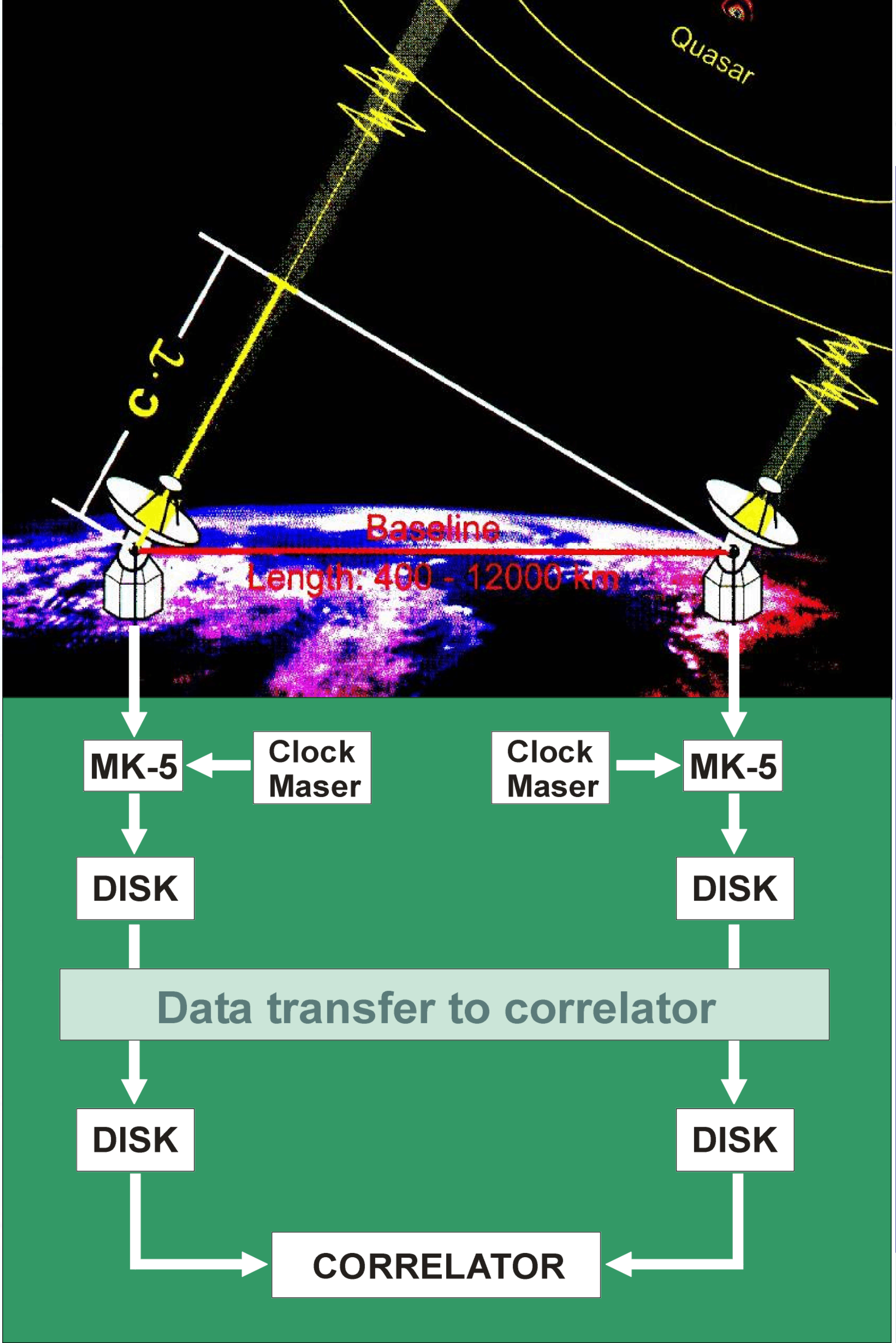


## 2.1. Measurement:

### Technical aspects of measurement

- Recording of radio signals
  - 8 channels X-band
    
    (8,4 GHz ~ 3,5 cm)
  - 6 channels S-band
    
    (2,3 GHz ~ 13 cm)
  - datastream 1 Gbit/s
  - Time & frequency
    - (DF/F ~ $10^{-15}$)
  - Data units
    - Magnetic tapes (until MK-4)
    - hard discs (from MK-5)
- Correlation
  - $\tau$ ~ 10 ....30 ps

# Basic equation

$$\tau = -\frac{1}{c}\mathbf{b} \cdot \mathbf{k}$$

b … baseline vector
k … source vector
*c* … velocity of light

$$\tau = -\frac{1}{c}\mathbf{b}\, WSNP \quad \mathbf{k}$$

<u>Transformation CRS → TRS:</u>

*W* … rotational matrix for polar motion
*S* … matrix for Earth's rotation (UT1)
*N* … Nutation
*P* … Precession

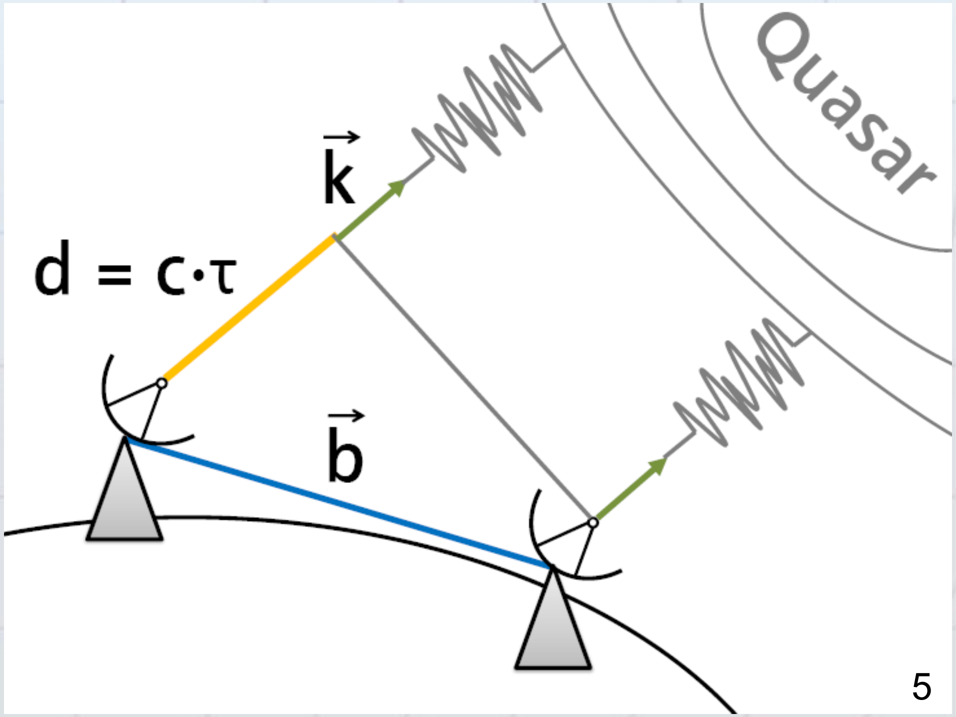

# Carrying out a VLBI-experiment

1. PLANNING
2. OBSERVATION
3. CORRELATION
4. ANALYSIS

### 3.1. Planning:

- Define a time schedule (*scheduling*)
- The schedule is decisive for the accuracy of the target parameters
- ~50 Stations, >1000 sources
- Scheduling is coordinated by the IVS
- Minimum 1 observation per parameter; in reality highly redundant
- E.g. ~100 observations per baseline

3.1.2. **VLBI Stations** (Components of the IVS))

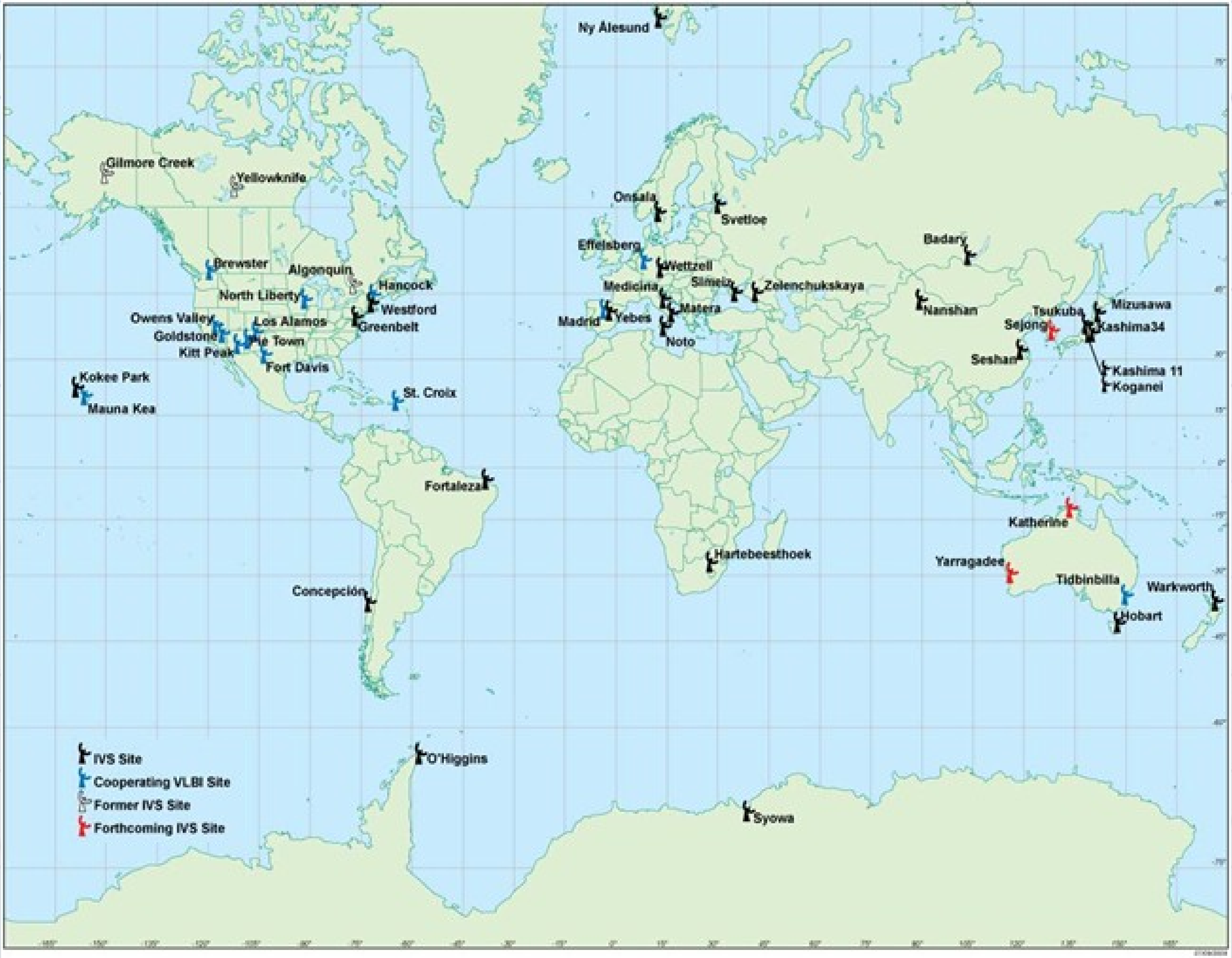

# Scheduling

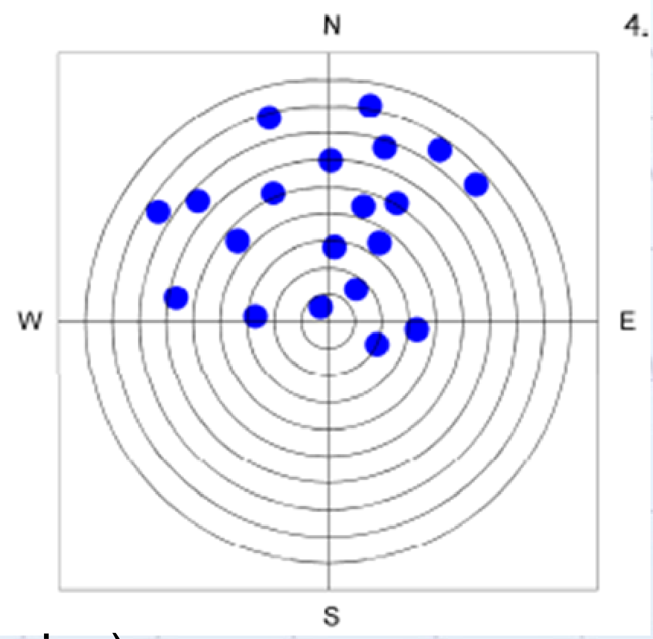


Depends on:

- observation window (sub-netting)
- predefined network
- goal of the session
- length of observation:  SNR = f(source, antenna size)
- spin velocities of the antennas
- optimization:
  - high number of observations
  - uniform sky coverage
  - short idling (energy!)
  - … ?
- the **scheduling problem is not fully solved!**

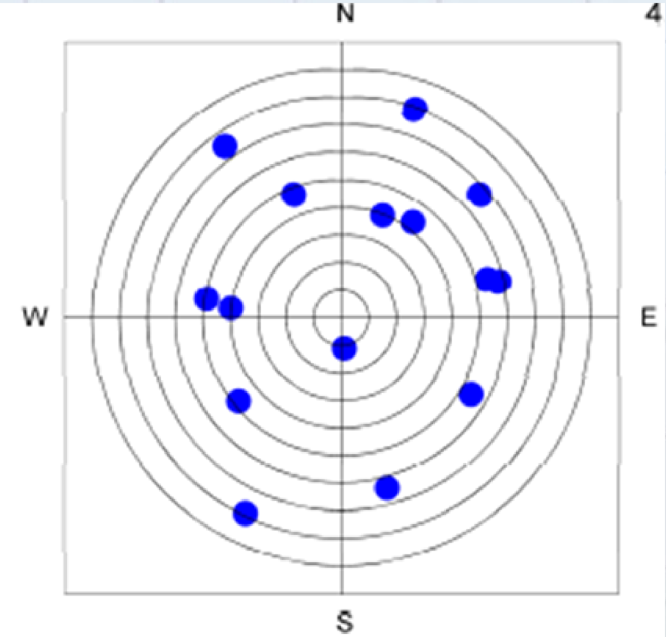

### 3.1.4 radio sources:

# ICRF-2

- since 08/2009
- 295 defining sources
- totally 3414 sources

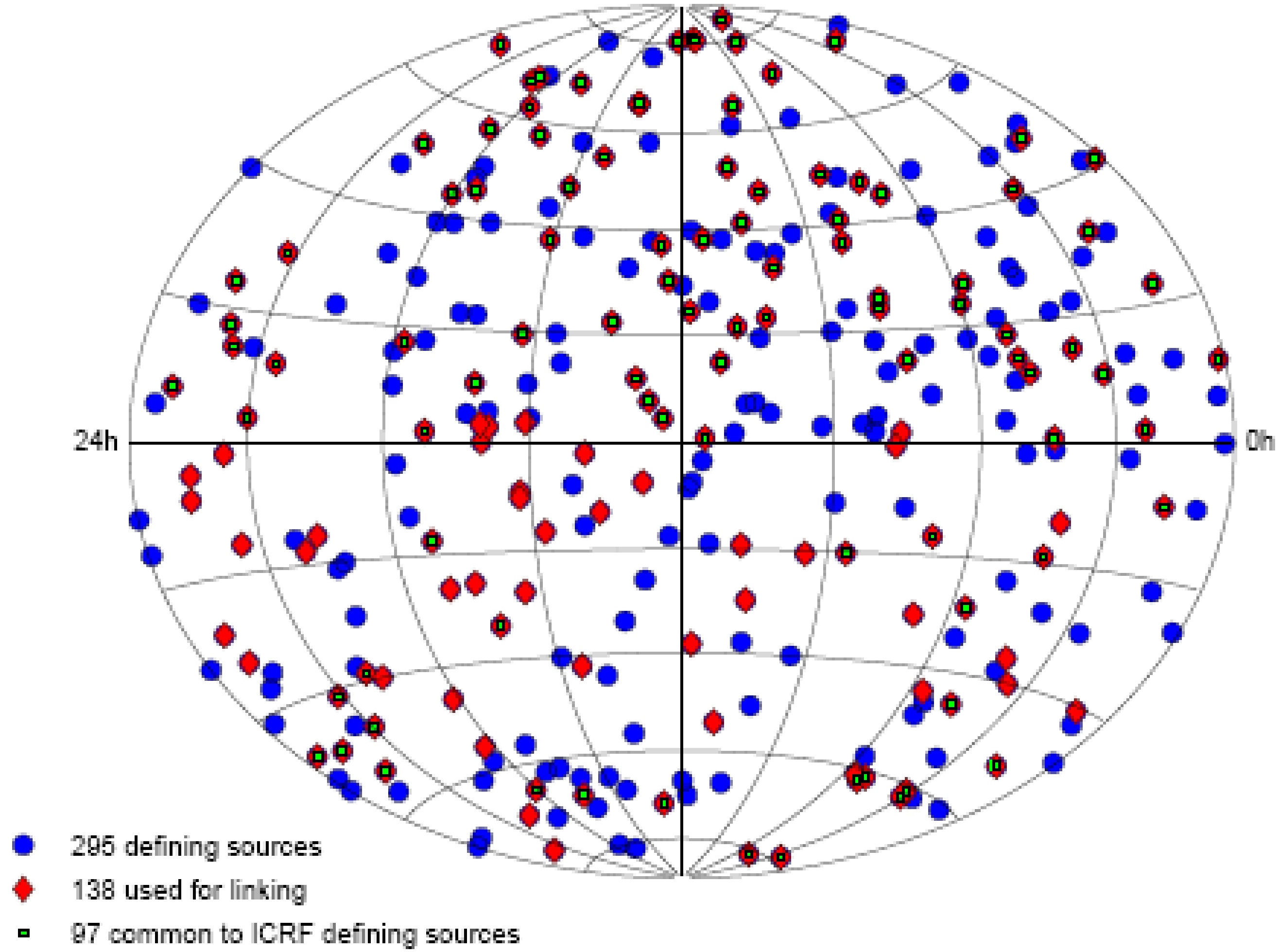


| ICRF Designation (1) | IERS Des. (2) | Inf. (3) | Right Ascension J2000.0 h m s | Declination J2000.0 o ' " | Uncertainty R.A. s | Uncertainty Dec. " | Corr. RA-Dc (4) | Mean MJD | First MJD | Last MJD | Nb sess. | Nb del. |
|---|---|---|---|---|---|---|---|---|---|---|---|---|
| | | | | | | | | of observation span | | | | |
| ICRF J000108.6+191433 | 2358+189 | | 00 01 08.62156690 | 19 14 33.8017390 | 0.00000490 | 0.0000984 | 0.080 | 53306.0 | 50085.5 | 54907.7 | 21 | 716 |
| ICRF J000211.9-215309 | 2359-221 | | 00 02 11.98262436 | -21 53 09.8359742 | 0.00115400 | 0.0386714 | 0.971 | 54818.7 | 54818.7 | 54818.7 | 1 | 3 |
| ICRF J000435.6-473619 | 0002-478 | D | 00 04 35.65550384 | -47 36 19.6037899 | 0.00001359 | 0.0002139 | 0.383 | 52501.0 | 49330.5 | 54670.7 | 28 | 129 |
| ICRF J000435.7+201942 | 0002+200 | | 00 04 35.75829931 | 20 19 42.3174919 | 0.00001434 | 0.0002426 | 0.079 | 52600.4 | 52409.7 | 52983.7 | 3 | 102 |
| ICRF J000557.1+382015 | 0003+380 | | 00 05 57.17539168 | 38 20 15.1489409 | 0.00000488 | 0.0000621 | -0.083 | 52010.2 | 48720.9 | 54718.7 | 26 | 1518 |
| ICRF J000613.8-062335 | 0003-066 | | 00 06 13.89288849 | -06 23 35.3353162 | 0.00000277 | 0.0000437 | -0.035 | 52342.2 | 47176.5 | 54889.8 | 1254 | 26713 |
| ICRF J000800.3-233918 | 0005-239 | | 00 08 00.36965673 | -23 39 18.1511374 | 0.00002400 | 0.0007055 | -0.650 | 50918.1 | 50632.3 | 54643.7 | 3 | 95 |
| ICRF J001031.0+105829 | 0007+106 | D | 00 10 31.00590186 | 10 58 29.5043827 | 0.00000491 | 0.0000930 | -0.187 | 53063.9 | 47288.7 | 54803.7 | 29 | 559 |
| ICRF J001033.9+172418 | 0007+171 | | 00 10 33.99063132 | 17 24 18.7613217 | 0.00000486 | 0.0000824 | -0.098 | 51780.9 | 47931.6 | 54844.7 | 40 | 1242 |
| ICRF J001052.5-415310 | 0008-421 | | 00 10 52.51790008 | -41 53 10.7781702 | 0.00019412 | 0.0043581 | -0.068 | 50998.2 | 48162.4 | 52409.7 | 5 | 22 |
| ICRF J001101.2-261233 | 0008-264 | D | 00 11 01.24673846 | -26 12 33.3770171 | 0.00000660 | 0.0000936 | -0.183 | 52407.5 | 47686.1 | 54768.6 | 45 | 592 |

# Radio source structure

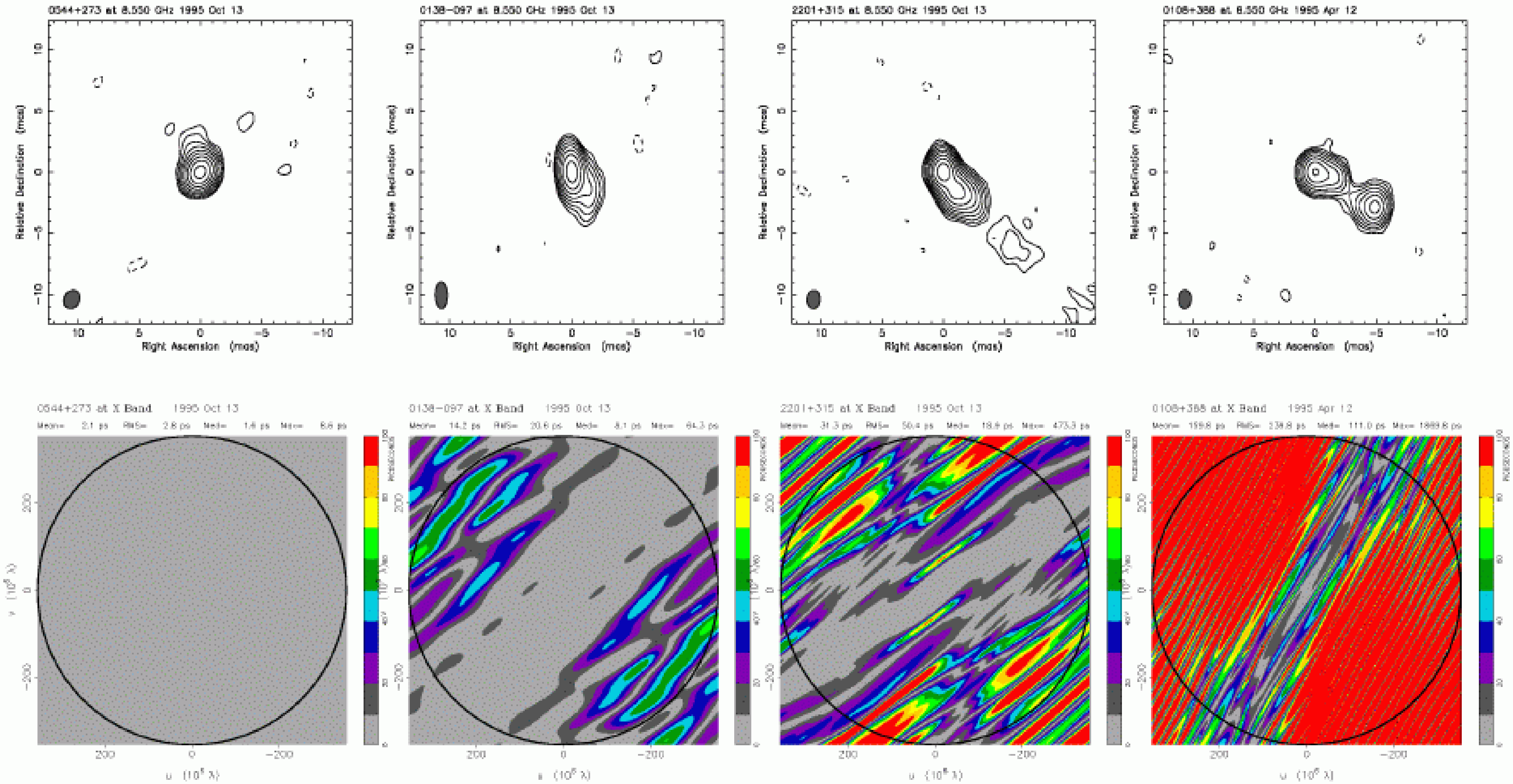


Structure Index

SI = 1 "excellent"

SI = 2 "good"

SI = 3 "poor"

SI = 4 "very poor"

# Frequency dependence of the point of maximal intensity

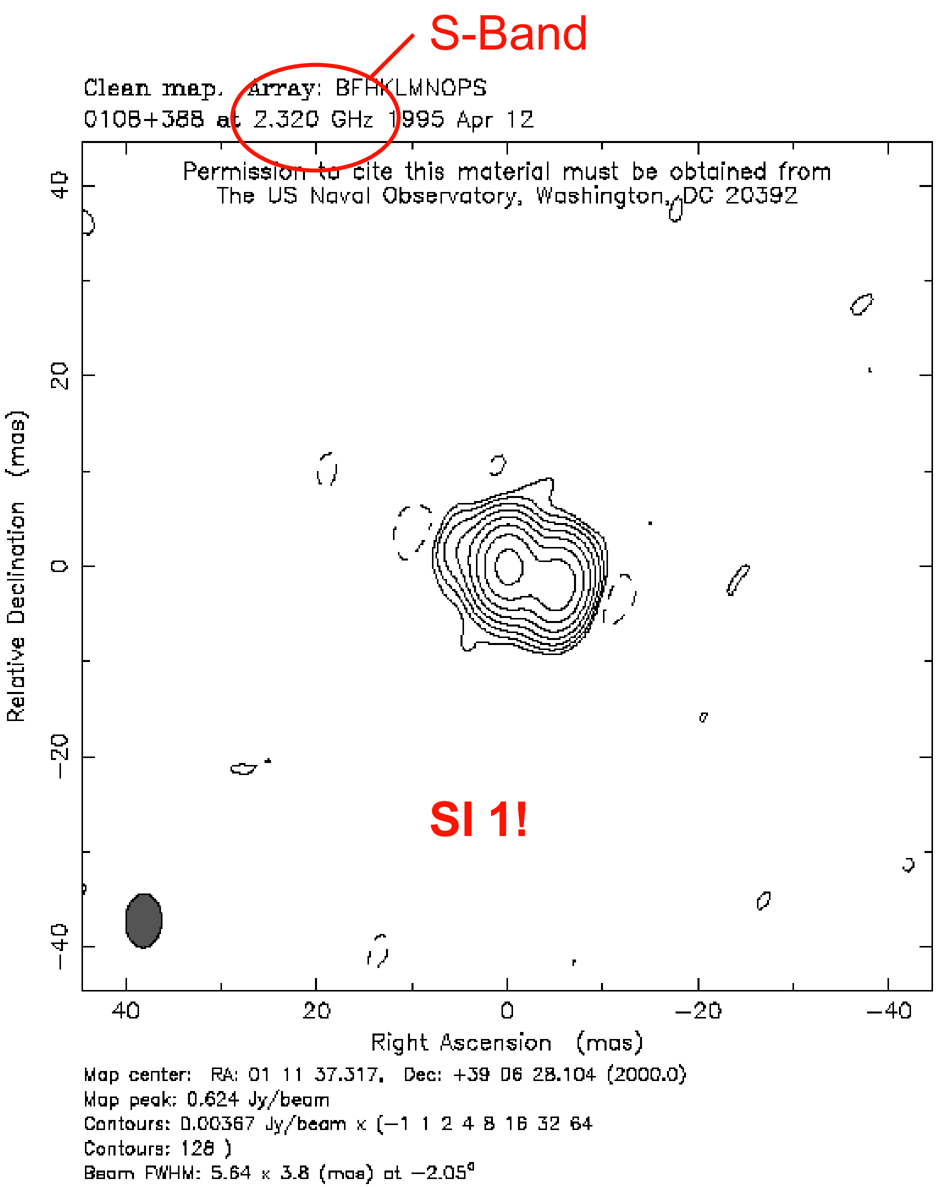


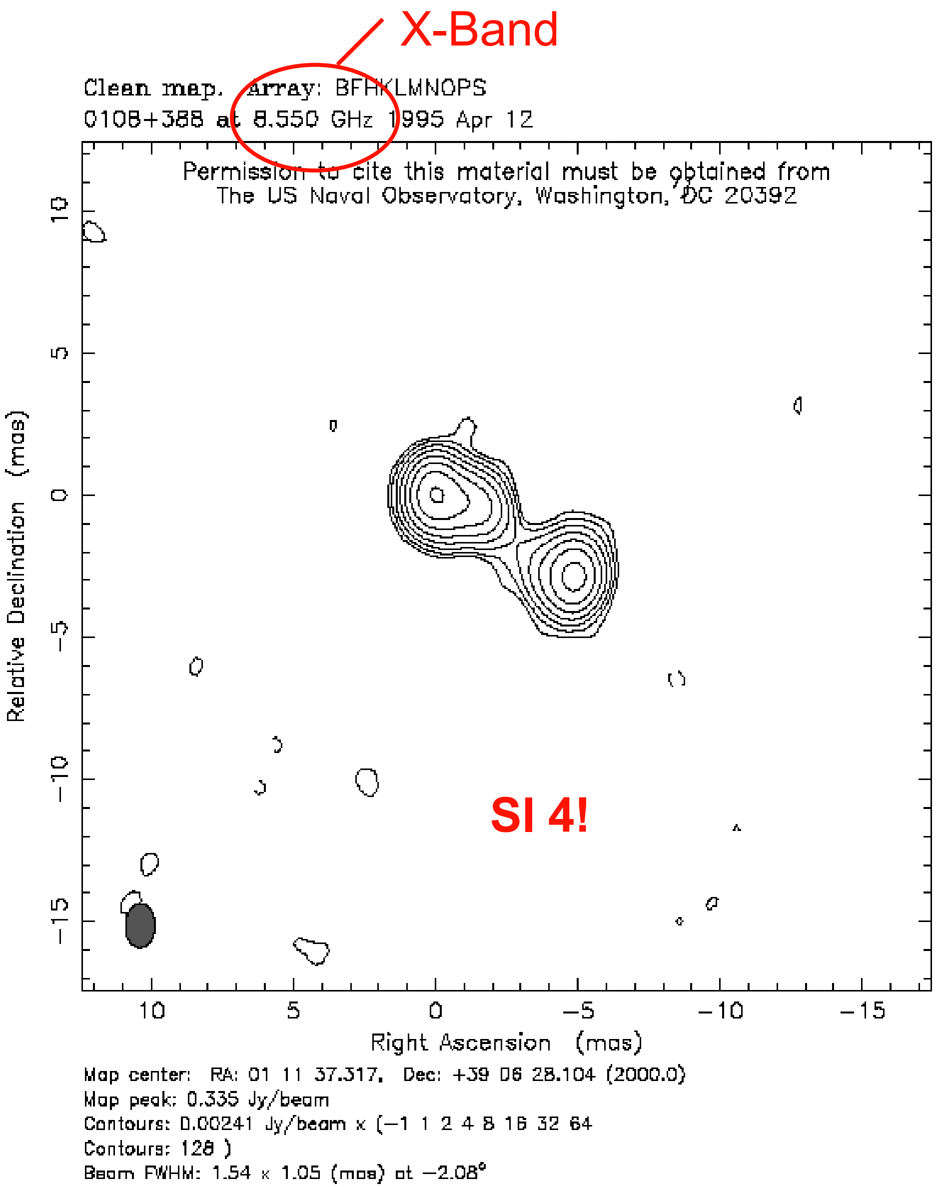

# SKED - file

Observing stations

Frequency bands

```
$SKED
0537-441   10 SX PREOB  10228170000       43 MIDOB          0 POSTOB H-A- 1F000000 1F000000 YYNN
1732+389   10 SX PREOB  10228170000      172 MIDOB          0 POSTOB J-O-B-CWE- 1F000000 1F000000
0016+731   10 SX PREOB  10228170247       43 MIDOB          0 POSTOB BWO-CW 1F000000 1F000000 1F0
2106+143   10 SX PREOB  10228170738      165 MIDOB          0 POSTOB H-OWBWC- 1F000000 1F000000 1
1124-186   10 SX PREOB  10228170746      206 MIDOB          0 POSTOB J-ACE- 1F000000 1F000000 1F0
0727-115   10 SX PREOB  10228171207       43 MIDOB          0 POSTOB ACE- 1F000000 1F000000 YYNN
0013-005   10 SX PREOB  10228171222       83 MIDOB          0 POSTOB OWH-C- 1F000000 1F000000 1F0
0955+326   10 SX PREOB  10228171327      237 MIDOB          0 POSTOB BWAC 1F000000 1F000000 YYNN
0234+285   10 SX PREOB  10228171539       43 MIDOB          0 POSTOB OWH-C- 1F000000 1F000000 1F0
0403-132   10 SX PREOB  10228171832      155 MIDOB          0 POSTOB H-OWA- 1F000000 1F000000 1F0
0133+476   10 SX PREOB  10228171931       43 MIDOB          0 POSTOB E-CWBW 1F000000 1F000000 1F0
0215+015   10 SX PREOB  10228172238       43 MIDOB          0 POSTOB OWC-H- 1F000000 1F000000 1F0
1324+224   10 SX PREOB  10228172510      110 MIDOB          0 POSTOB J-B-ACE- 1F000000 1F000000 1
0104-408   10 SX PREOB  10228172517       43 MIDOB          0 POSTOB H-OWC- 1F000000 1F000000 1F0
0657+172   10 SX PREOB  10228172812      217 MIDOB          0 POSTOB ACE- 1F000000 1F000000 YYNN
```

Observed source

time [yy dd hh mm ss]
day of year: 228 (=17. Aug.)

## 3.2. Observation:

- Variation of the interference due to Earth rotation, *fringe frequency f(t)*:

$$f(t) = \frac{1}{2\pi}\frac{d\Phi(t)}{dt}$$

$\Phi(t)$... Phase difference of the observed radiation

- Phase meas.:

$$\Phi(t) = -2\pi\frac{f}{c}\cos\psi(t)\cdot b$$

$f$ ... frequency

$b$ ... baseline

$\psi(t)$... angle between *b* and source direction

- →

$$d(t) = c\cdot\frac{\Phi(t)}{2\pi f} + N\cdot\lambda$$

$d(t)$... travelled distance of the signal ('group delay')

$N$ ... integer number of multiples

$\lambda$ ... wavelength

- 
- → Phase stability (technical issue)

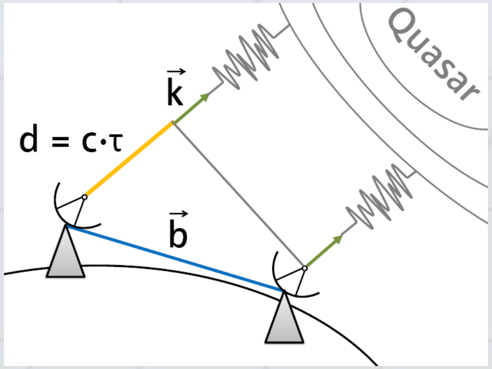

# Resolving the ambiguities

- **Depends on the wavelength and the length of the baseline**
  **→ longer baselines & higher frequencies need better a priori models**
- **Short baselines: phase delay solution is already possible**
- **Long baselines: group delay solution (= derivative of the phase w.r.t. frequency)**

$$\tau = \frac{d\Phi}{d\omega}$$

- **Replace $\Phi$ by the station dependent source vector *k* and $\omega = 2\pi f$:**

$$\tau(t) = -\frac{\vec{k} \cdot b(t)}{c} + \textit{instrumental und atmospheric errors}$$

**… basic equation of VLBI**

# Sensitivity of the VLBI system

$$SNR = \eta \frac{F_d}{2k} \sqrt{\frac{A_1 \cdot A_2}{T_{S_1} \cdot T_{S_2}}} \cdot \sqrt{2BT}$$

**10 < *SNR* < 100**

$SNR$ … signal to noise ratio

$\eta$ … factor representing energy loss due to digitalization, filtering, …

$F_d$ … flow density of the source [Janksy] $1\,Jy = \frac{1 \cdot 10^{-26}\,W}{m^2\,Hz}$

$k$ … Boltzmann constant $E_{kin} = \frac{1}{2} k \cdot T$

$A_1, A_2$ … effective diameter of the antenna (geom. diameter * efficiency) A1=20m, A2=20m ↔ A1=10m, A2=40m ↔ A1=4m, A2=100m

$T_{S_1}, T_{S_2}$ … noise temperature of the receivers [Kelvin], nowadays: 40-50 K

$B$ … bandwidth of the receiving system

$T$ … coherent time of integration [< 10 min] (=time of one scan)

## 3.2. Observation:

# Accuracy of VLBI group delay measurement

**a) single band delay:**

$$\sigma_t = \pm \frac{1}{2\pi} \cdot \frac{1}{SNR \cdot B}$$

with bandwidth

$$\left.\begin{aligned} B &= 2\,MHz \\ SNR &\approx 18 \end{aligned}\right\} \Rightarrow \sigma_t \approx \pm 50\ cm$$

**b) multi band delay (e.g. X-Band, 8 x 2 MHz):**

covered bandwidth $\Delta B = f_{\max} - f_{\min}$

effective bandwidth $B_{eff} = \sqrt{\frac{\Sigma(f_i - f_m)^2}{N}}$

*N* – number of channels

$f_m$ – mean frequency

**Bandwidth synthesis:** it is not necessary to cover the whole bandpass with frequencies; instead, it is enough to record signals at the edges and on certain channels in between.

$$\sigma_t = \pm \frac{1}{2\pi} \cdot \frac{1}{SNR \cdot B_{eff}}$$

(Example: MkIII, X-Band, ΔB=360 MHz, $B_{eff}$=140,22 MHz)

**c) Examples:**

$$F_d = 1\,JANSKY,\ d_1, d_2 = 30\ m,\ Effciency = 50\ \%,\ T = 300\ \sec$$

$$T_{S_1}, T_{S_2} = 160\ {}^\circ K\ (uncooled),\ B_{eff} = 140{,}22\ MHz \Rightarrow SNR \approx 27 \Rightarrow \sigma_t = \pm 0{,}041\ n\sec(= 1{,}4\,cm)$$

$$T_{S_1}, T_{S_2} = 60\ {}^\circ K\ (cooled),\ B_{eff} = 140{,}22\ MHz \Rightarrow SNR \approx 75 \Rightarrow \sigma_t = \pm 0{,}013\ n\sec(= 0{,}4\,cm)$$

## 3.2.1 Signal:

- **'Geodetic' frequencies in the range 0.4-30.0 GHz (100 GHz in astronomy)**
- **Standard since 1979: S-band: 2.3 GHz (13 cm), X-band: 8.4 GHz (3.5 cm)**
- **We are observing only slight deviations (0.1%) from the general background noise of the sky**

| | |
|---|---|
| Radioloud Sun | 100.000.000 Jy |
| Quiet Sun | 100.000 Jy |
| SNR Cassiopeia A | 3.400 Jy |
| Radiogalaxy Cygnus A | 2.200 Jy |
| Cell phone on Moon | 1.000 Jy |
| M1 = Taurus A | 900 Jy |
| Usual radio sources | 0.1 – 10 Jy |

***Radio intensities for some transmitters on the northern sky at 900 MHz***

## 3.2.2 Instruments:

- As big as possible (good SNR)
- Surface accuracy 1/20 of the wavelength

  → 8,4 GHz → 3,6 cm → 5% = 1,8 mm
- Moving main reflector, with feed horn in the primary/secondary focus (with subreflector)

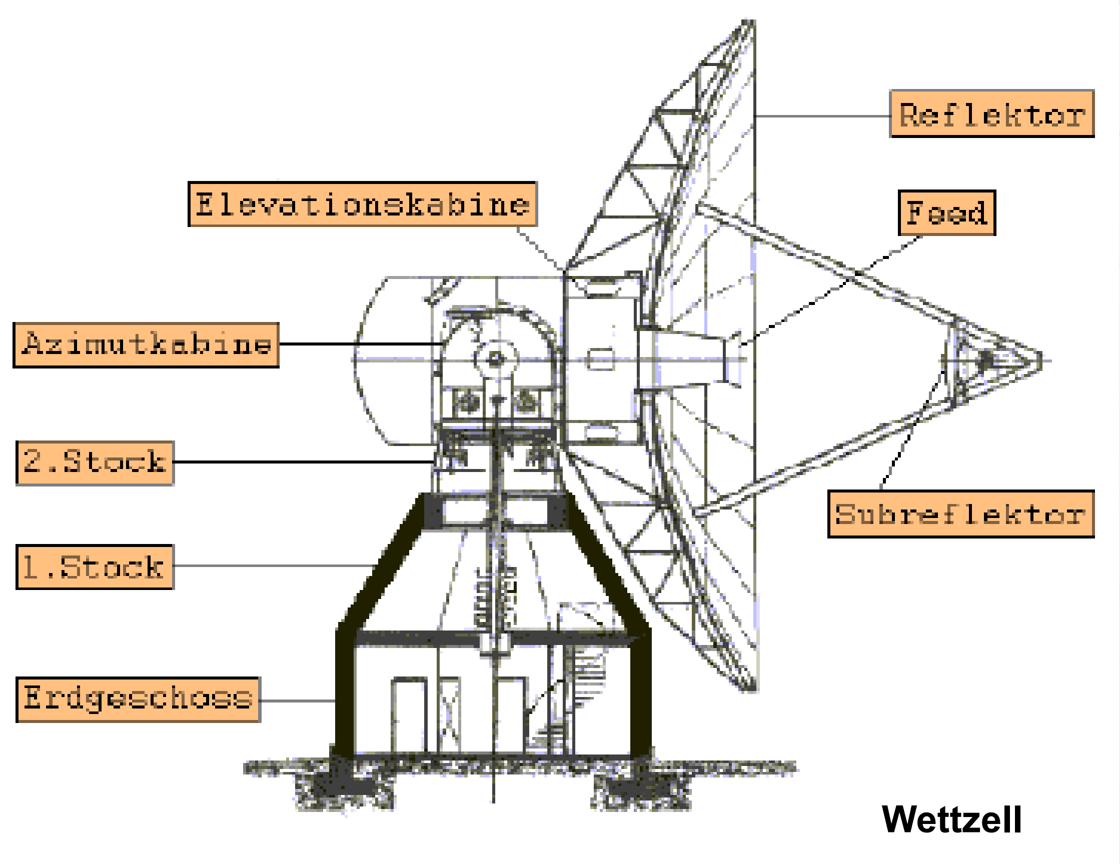

3.2.2 Instruments:

- **Reference point**

- Reference for group delays : Intersection between azimuth and elevation axis
- Path length form radio reference point to geometric reference point is calibrated by cable cal measurement

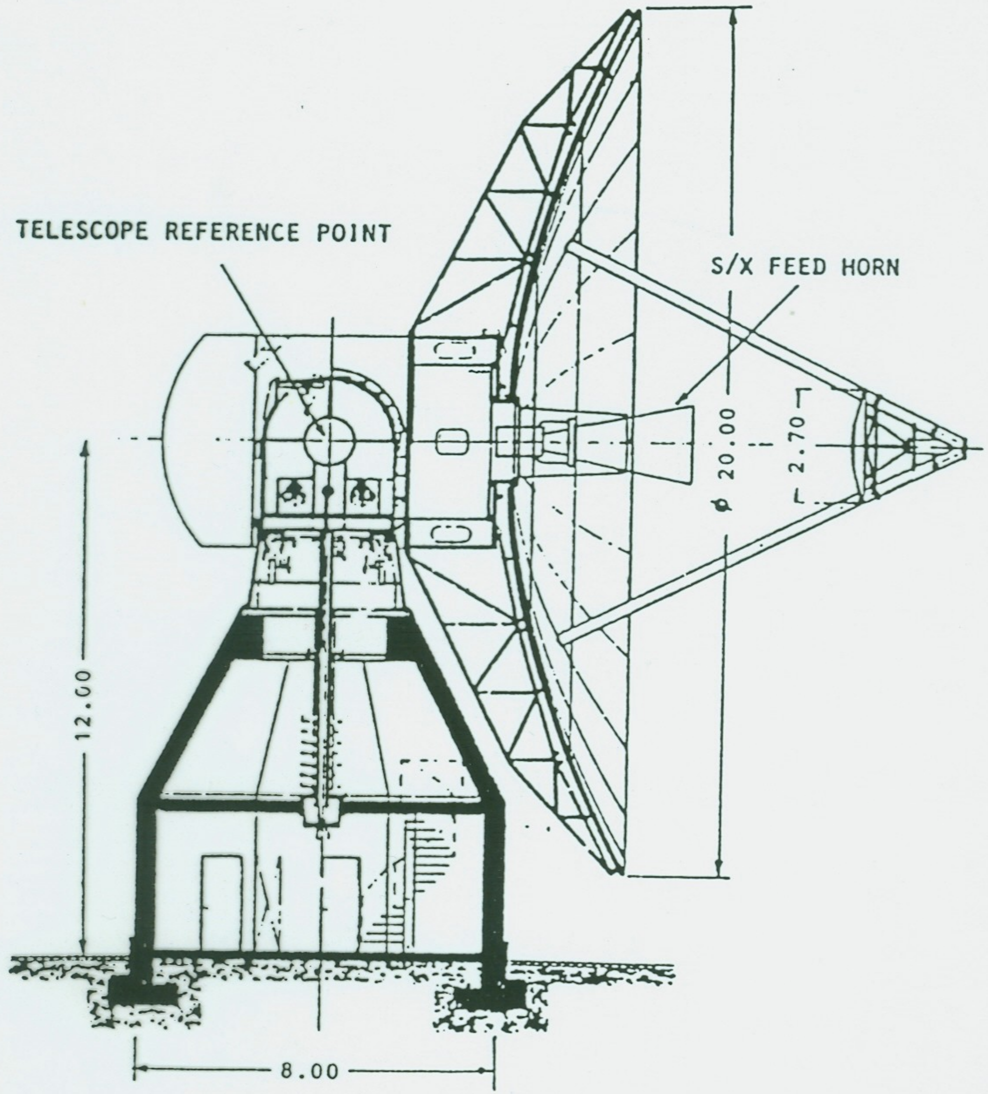


Fig. 9. The 20 m radiotelescope of the geodetic fundamental station Wettzell, Bavaria, Germany

**3.2.2 Instruments:**

- **critical: - external influences (Sun, temperature, wind)**
  **- self-gravitation**

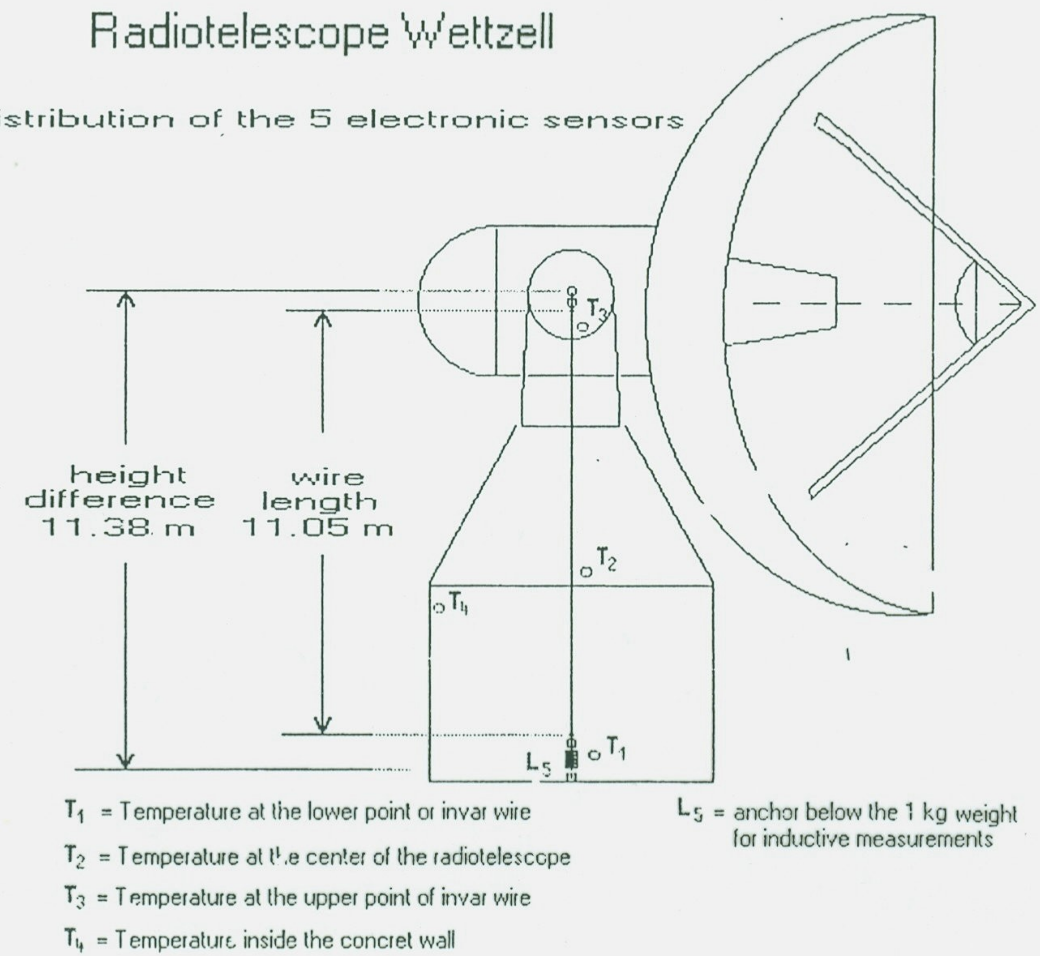


*Principle of Measurements.*

Ex.: temperature sensors on the telescope Wettzell

26.2.1997 — Invar measurements (hourly scan) of the height of the radiotelescope in Wettzell — 11.3.1998

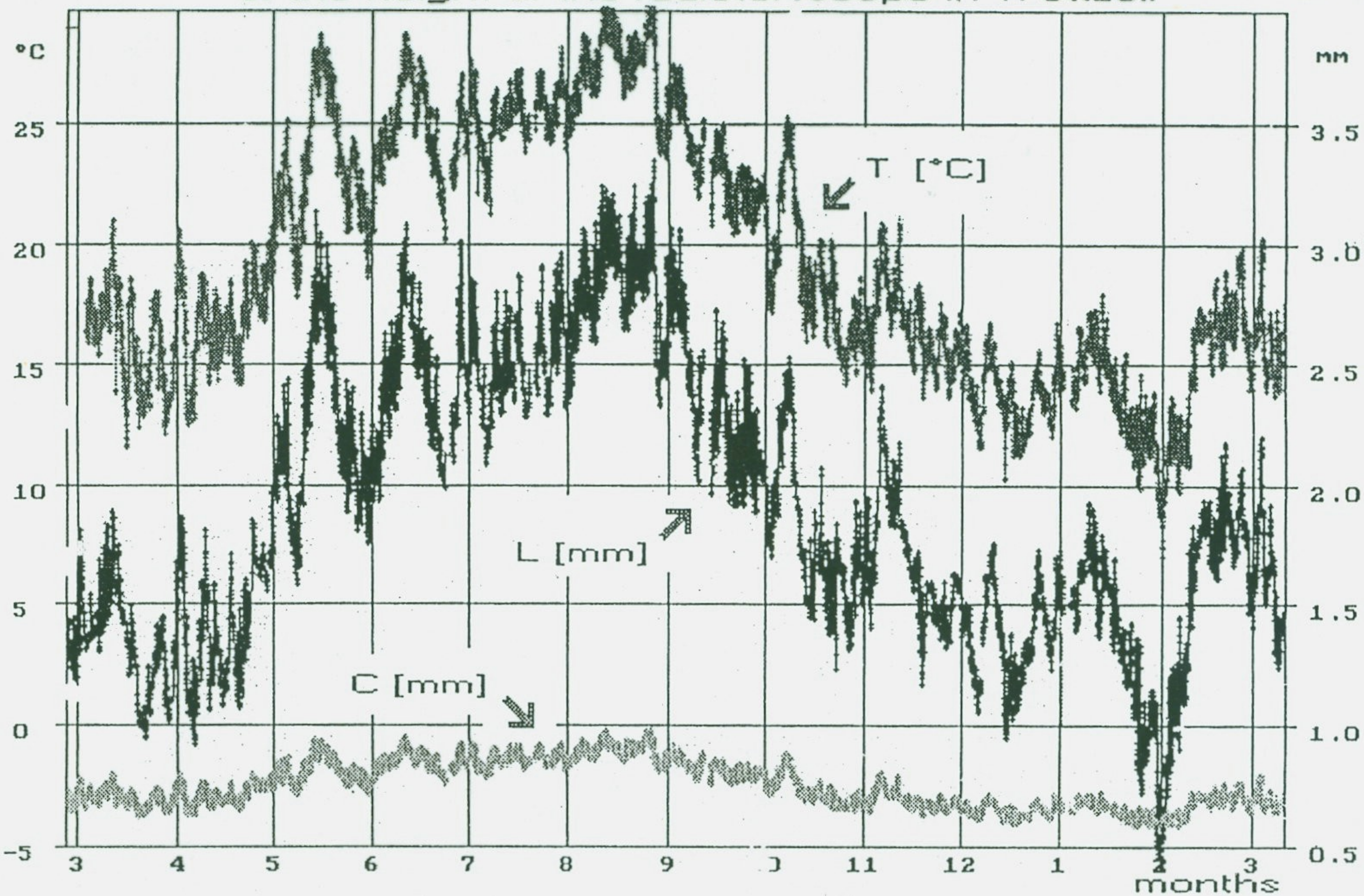


T [°C] = Temperature in the center of the radiotelescope
L[mm] = Height variations measured with invar
C[mm] = Correction due to temperature of invar wire

(Zernecke, 1999)

### 3.2.2 Instruments:

- critical: - external influences (Sun, temperature, wind)
  - self-gravitation
- radome
- Log-file: temperature, air pressure, humidity
- aims:
- high speed,
- high SNR,
- high sensitivity,
- sufficient surface accuracy

Onsala Space Observatory (20m)

## 3.2.3 Technical realization:

- After the signals enter the feed, they are sparated into two bands

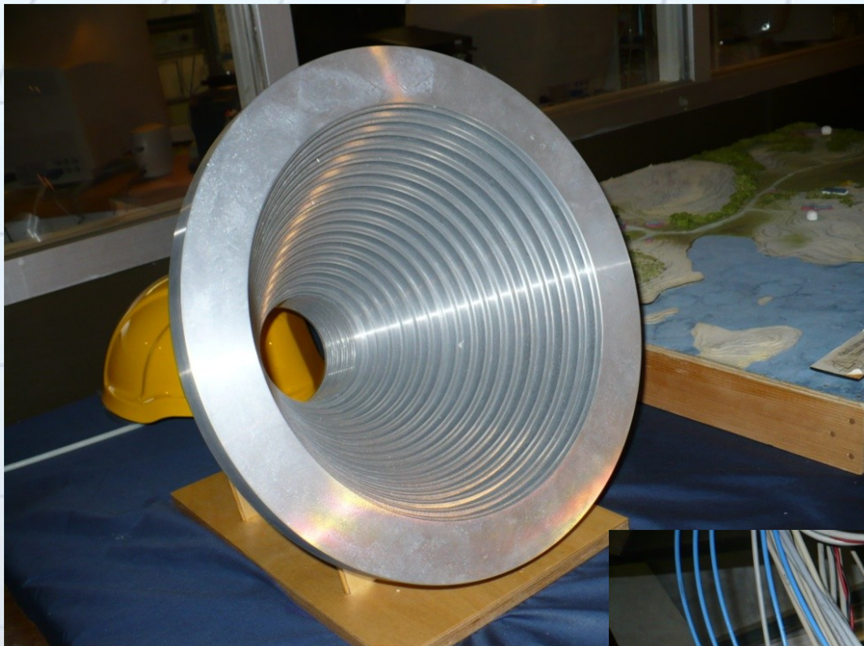

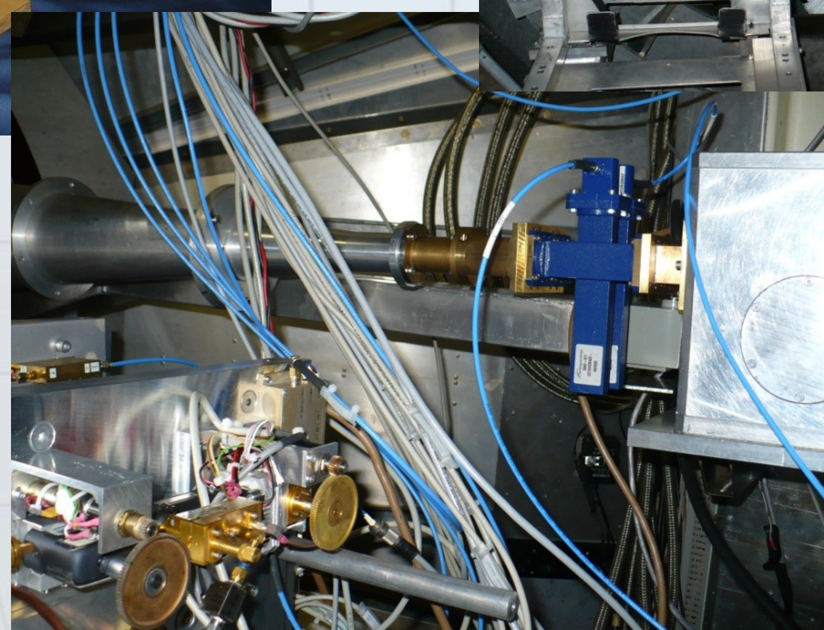

[Onsala]

### 3.2.3 Technical realization:

- 2 frequency bands
  → dispersive influences (Ionosphere)

$$\Delta \tau_x^{ion} = (\tau_x - \tau_s) \cdot \frac{f_s^2}{f_x^2 - f_s^2}$$

- Processing on two separate routes
- Down-converted on a bandwidth of 400 MHz (today ~700 MHz)
- Phase-stable down-converting with a local oscillator (gets its signal from the H-maser)

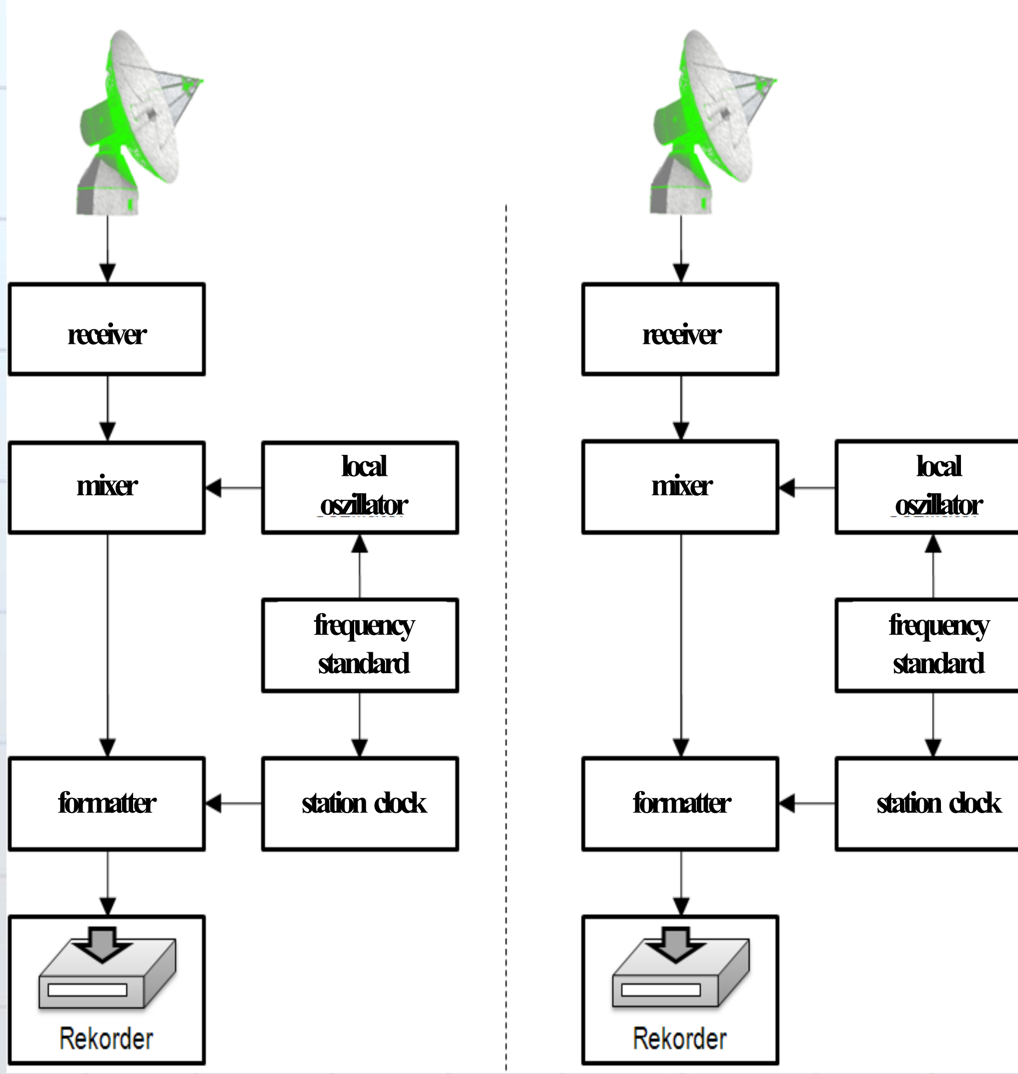

## 3.2.3 Technical realization:

- Several channels, each covering 2 MHz (high synthetic bandwidth)

680 MHz

| X-Band | S-Band |
|---|---|
| 8182,99 MHz | 2212,99 MHz |
| 8222,99 MHz | 2222,99 MHz |
| 8422,99 MHz | 2257,99 MHz |
| 8562,99 MHz | 2297,99 MHz |
| 8682,99 MHz | 2317,99 MHz |
| 8782,99 MHz | 2322,99 MHz |
| 8842,99 MHz | |
| 8862,99 MHz | |

X-Band und 6 S-Band Frequenzbänder des Mk 4 Systems

H-Maser

- Formatter:
  - Digitizes the signals
  - Time stamp from station clock (time of reception)
  - Writes data on magnetic bands/discs

## 3.2.3 Technical realization:

- **Shipping by airplane to the correlator**
- ***e-transfer*: 1st step to *real time* VLBI**

  **currently: only for *Intensives* (turnaround time: a few hours)**
- **Extremely high data rate: 512 Mb/sec resp. 1 Gb/sec; too large for the internet; data transfer via broadband communication networks**


Real-time e-VLBI demo at Super Computer Conference (Whitney 2005)

# e-VLBI Intensives (1h)

- Ultra-rapid Intensives between Europe and Japan

- Onsala-Tsukuba
  Metsähovi-Kashima

- UT1 – solution
  < 30 min.

21. Feb. 2008:
Results within 4' after the last scan [Matsuzaka et al., 2008]

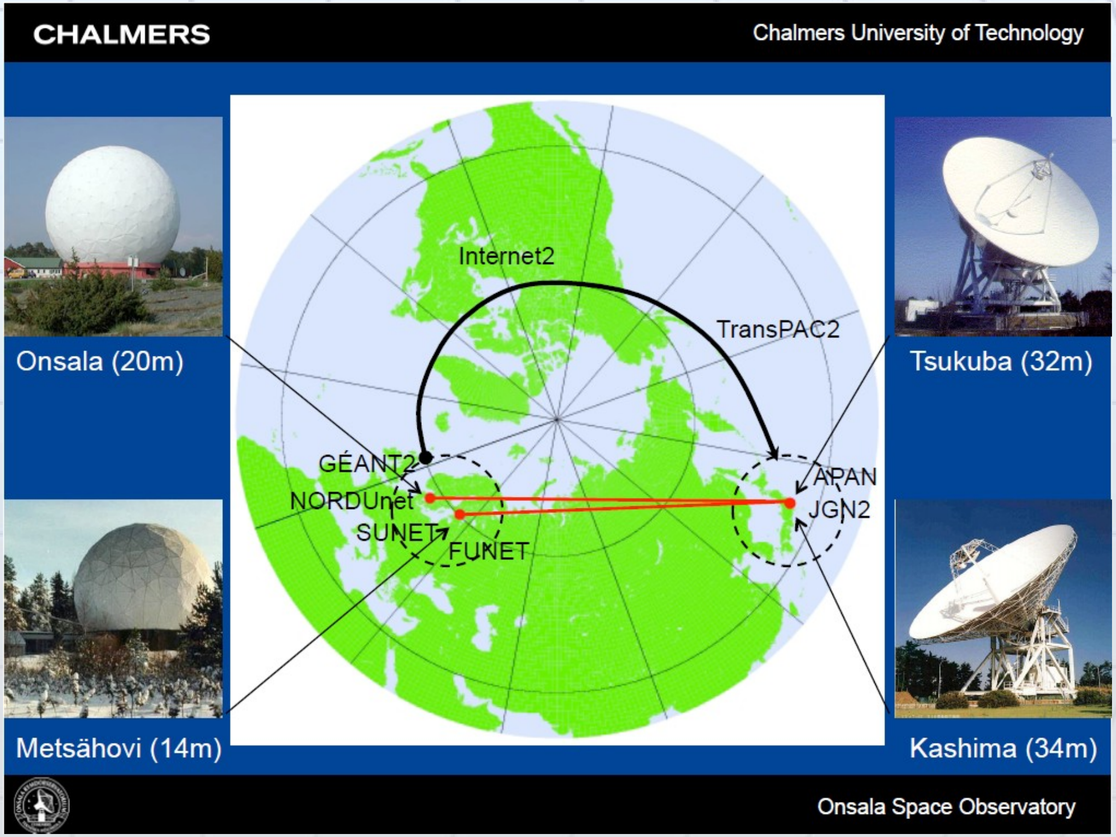


**[Haas et al., 2011:
Ultra-rapid dUT1-observations with e-VLBI]**

## 3.2.4 Instrumental erros:

- Differences in the signal path between receiving (arrival at the antenna) and the input of the time stamp
- Cable: strain, temperature
- Delay calibration system: test-signal
- Sign?: cable calibration (1 µsec)
- Phase calibration: calibration necessary for each channel
- Deformation of the antenna:
    - gravitation
    - wind pressure
    - temperature

→ Models (e.g. thermal antenna deformation)

### 3.2.4 Instrumental errors:

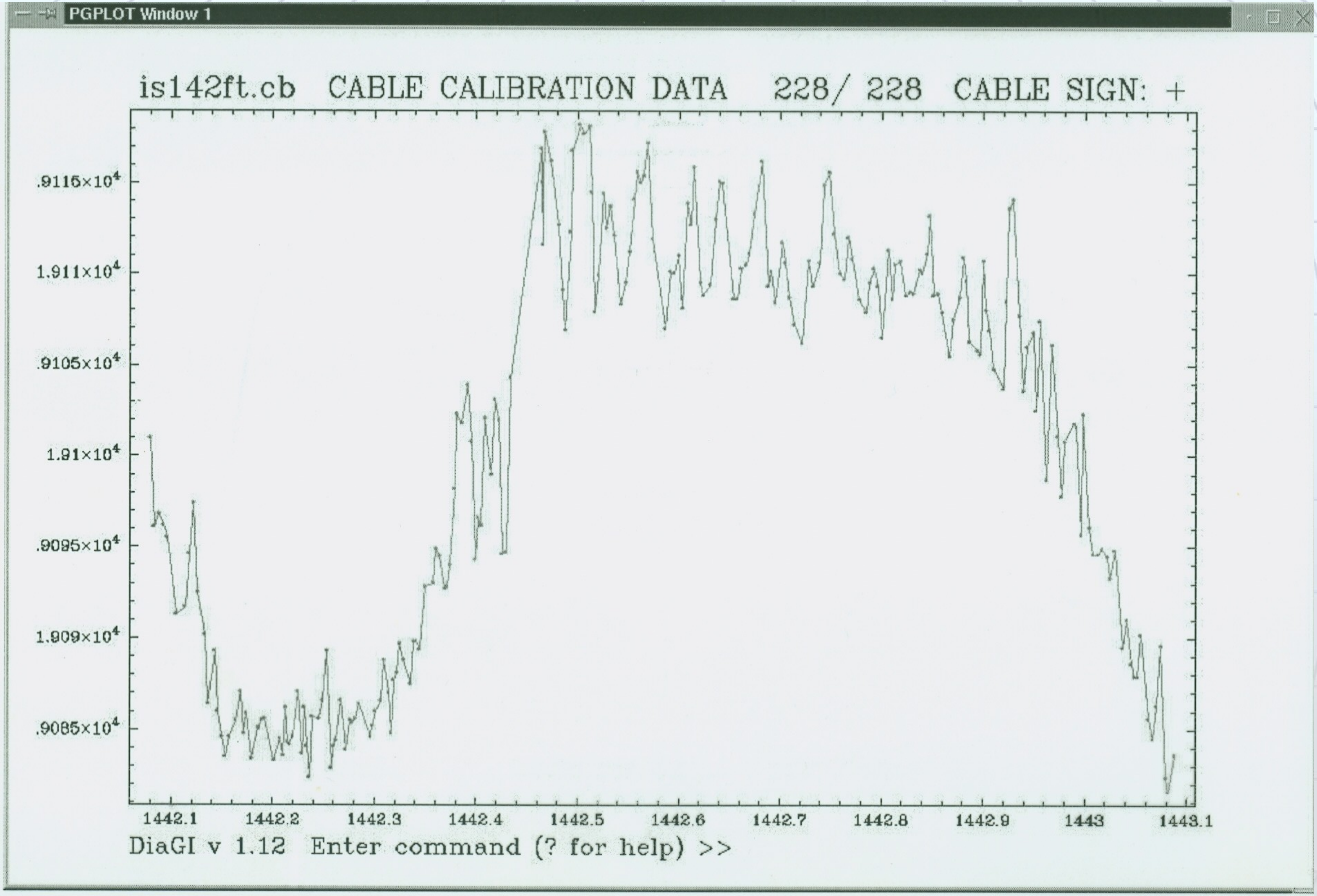

## 3.2.4 Instrumental errors:

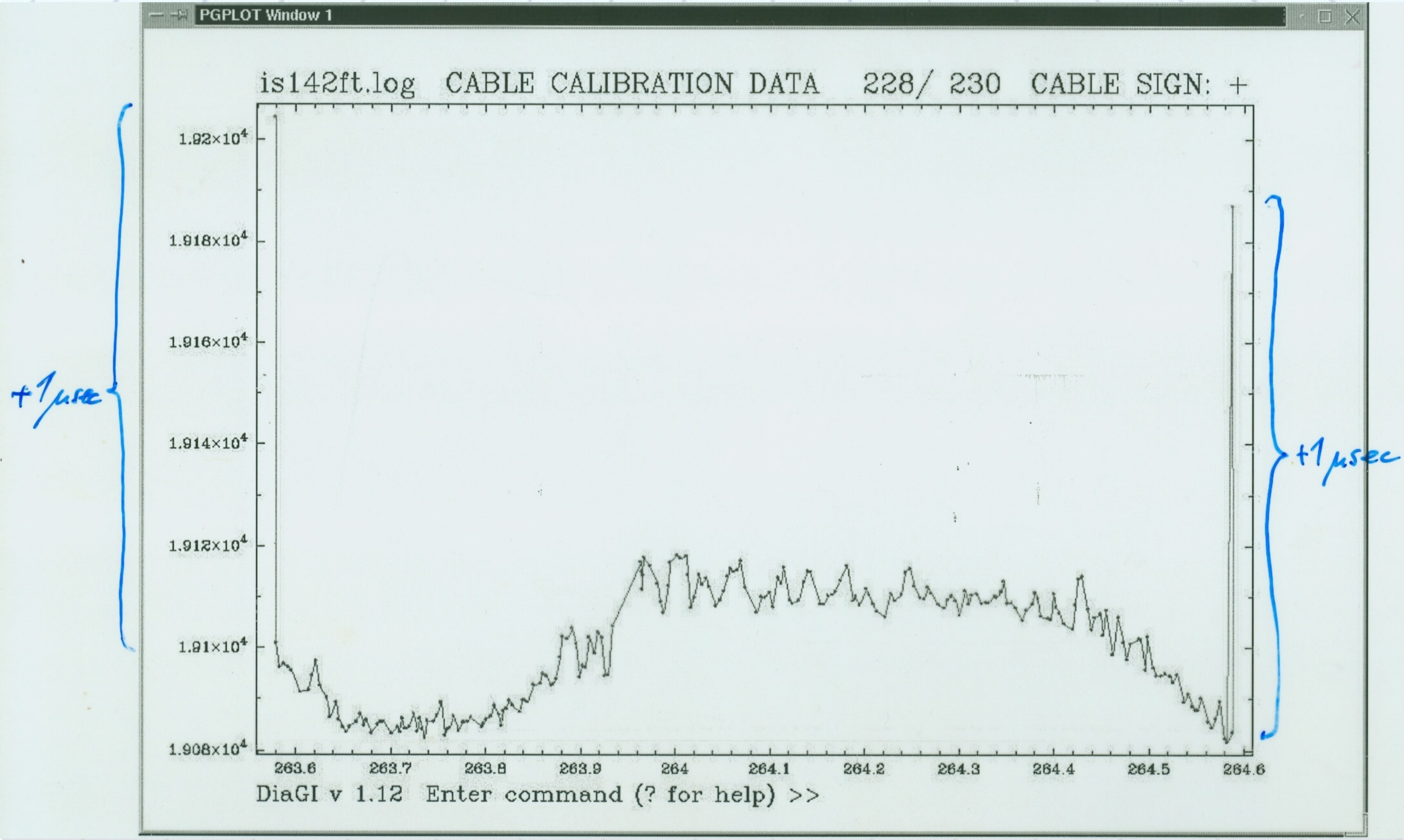

## 3.3 Correlation:

- **Correlation function:**

$$C_{\max} = \Sigma_{i=1}^{N} y(t_i)\,x(t_i - \tau)$$

Correlator:
Indentifying two identical signal components is successful, when the correlation amplitude is above a certain noise-level.
A-priori values are needed for
- station positions
- source positions
- clock rate differences

to calculate theoretical delays. This gives a search window of a few µsec for the correlation.

- **Differential Doppler shift due to Earth rotation (fringe stopping)**

→ **second observable** $\dot{\tau}$

## 3.3 Correlation:

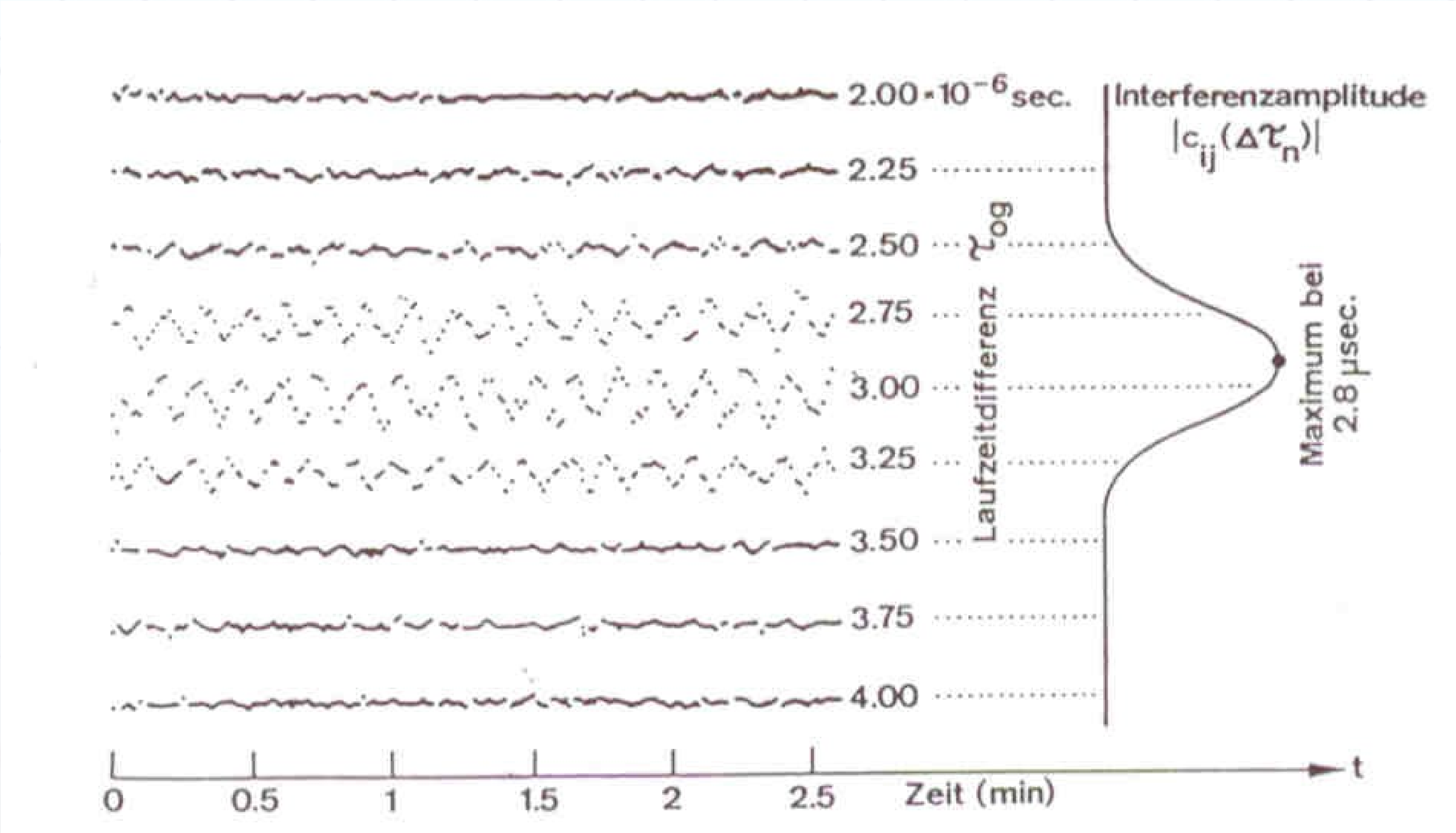


**Correlator output signal, maximum at τ**

**Signal is shifted for 0,25 µs; amplitude is shown at the right; there, a sinx [x] function is fitted, then the maximum is determined.**

## 3.4 Analysis:

# Geodetic analysis

- Determination of the theoretical delay with a priori station positions and source coordinates, with actual Earth orientation and by correcting for local and global (tidal) deformations.
- Comparison with the measured time delay (observed minus computed)
- Adjustment procedure (e.g. least-squares)
- Solving for global and/or local parameters

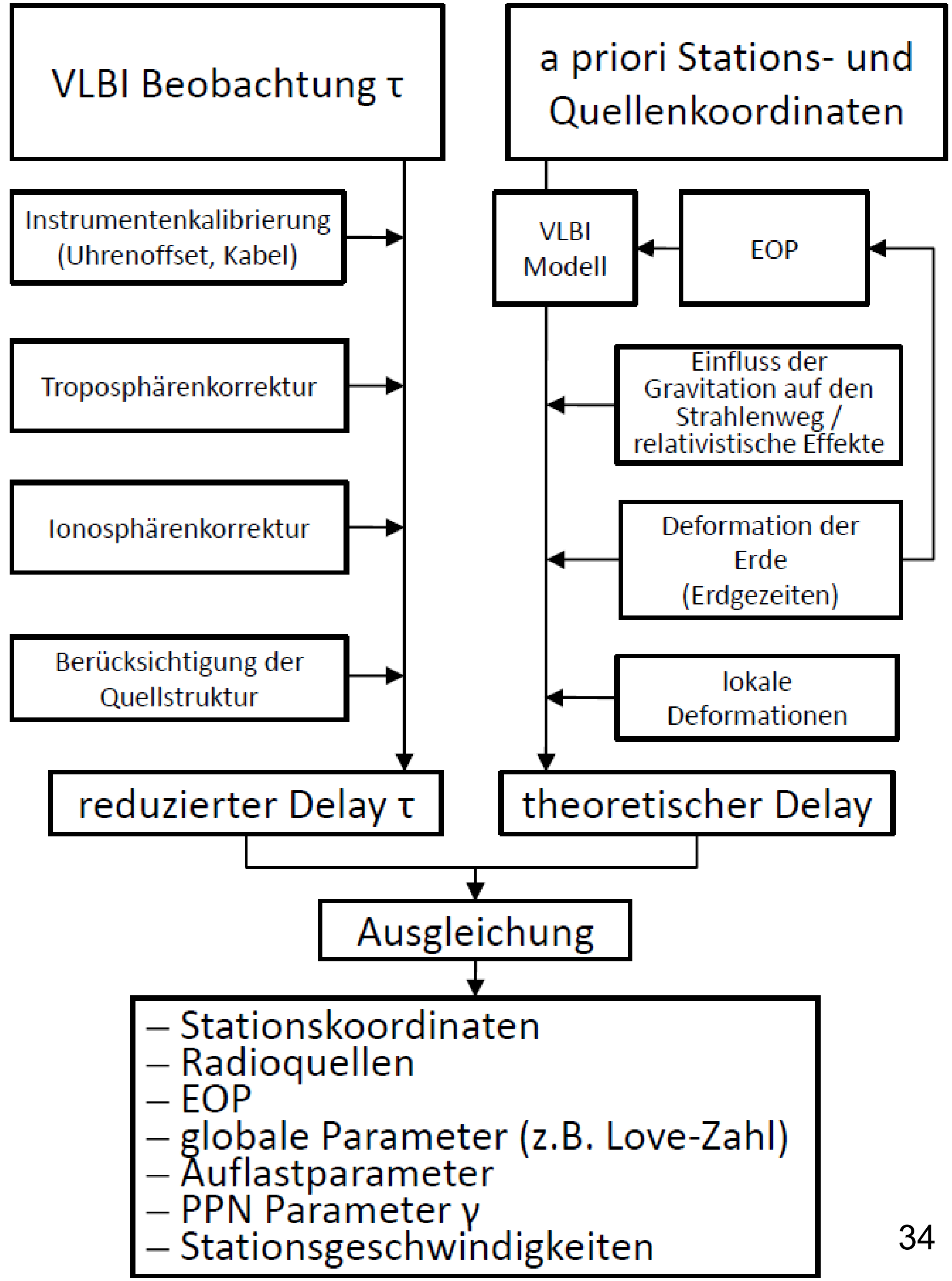

## Size of corrections & error model

| Modellkomponente | maximaler delay | derzeitiger Fehler |
|---|---|---|
| **BASISLINIE** | | |
| Geometrie | 6000 km | ... |
| Erdorbit (Abberation) | 600 m | 1 mm |
| Gravitativer delay | 2 m | 2 mm |
| **STATIONSPOSITIONEN** | | |
| Tektonik | 10 cm | 1 mm |
| Gezeiten | 50 cm | 3 mm |
| weitere Stationsbewegung | 5 cm | 5 mm |
| **ERDORIENTIERUNG** | | |
| UT1, Polbewegung | 20 m | 2 mm |
| Nutation/Präzession | 300 m | 3 mm |
| **RADIOQUELLENSTRUKTUR** | 5 cm | 10 mm |
| **ANTENNE** | 10 m | 10 mm |
| **INSTRUMENTENFEHLER** | 300 m | 5 mm |
| **ATMOSPHÄRE** | | |
| Ionosphäre | 1 m | 1 mm |
| Troposphäre | 20 m | 20 mm |

[Sovers et al., 1998]

# Ex.: 1 baseline (WEST-WETT), 14 days VieVS Delay

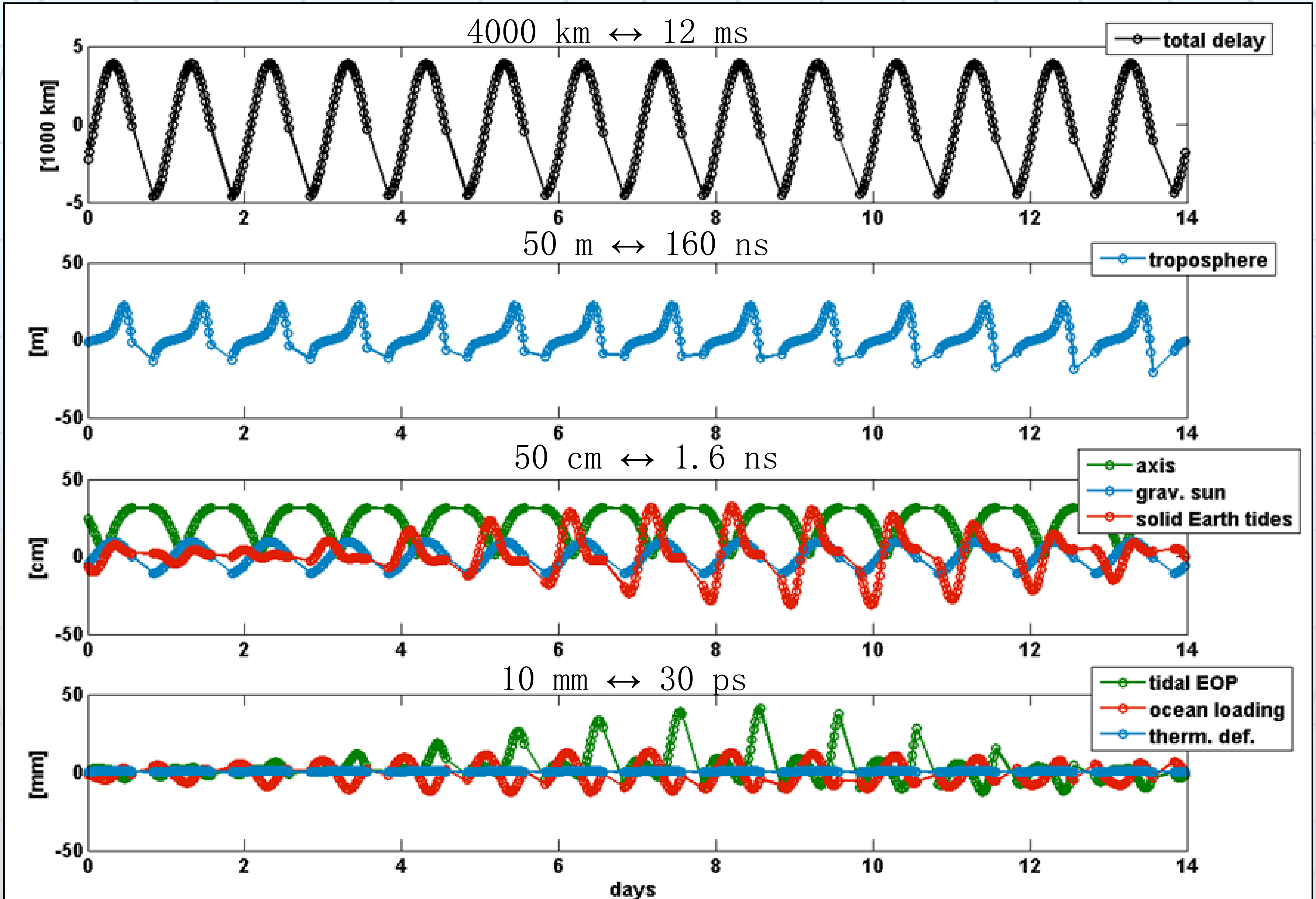

# Ocean loading

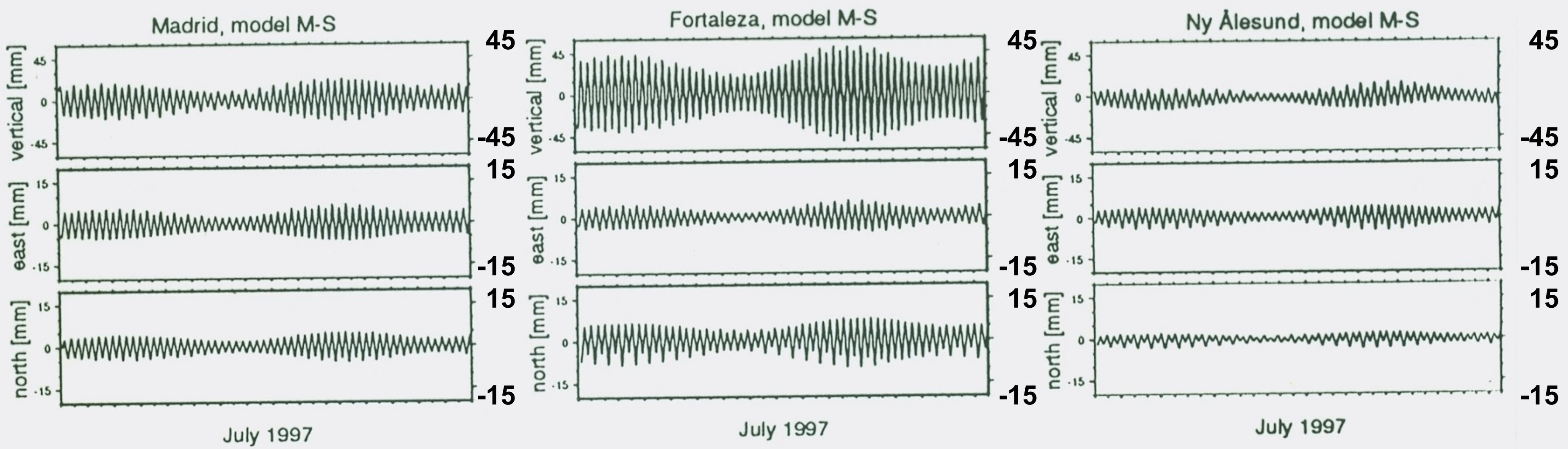


Ocean loading effetcs during July 1997 calculated for the inland site Madr (Spain), the coastal site Fortaleza (Brazil) and the island site Ny Ålesund (Spit bergen, Norway) with model M-S [SCHERNECK, 1991].

# Atmospheric loading

## Radiale Verschiebungen von VLBI-Stationen aufgrund atmosphärischer Auflasten

(Modell: MANABE et al., 1991)

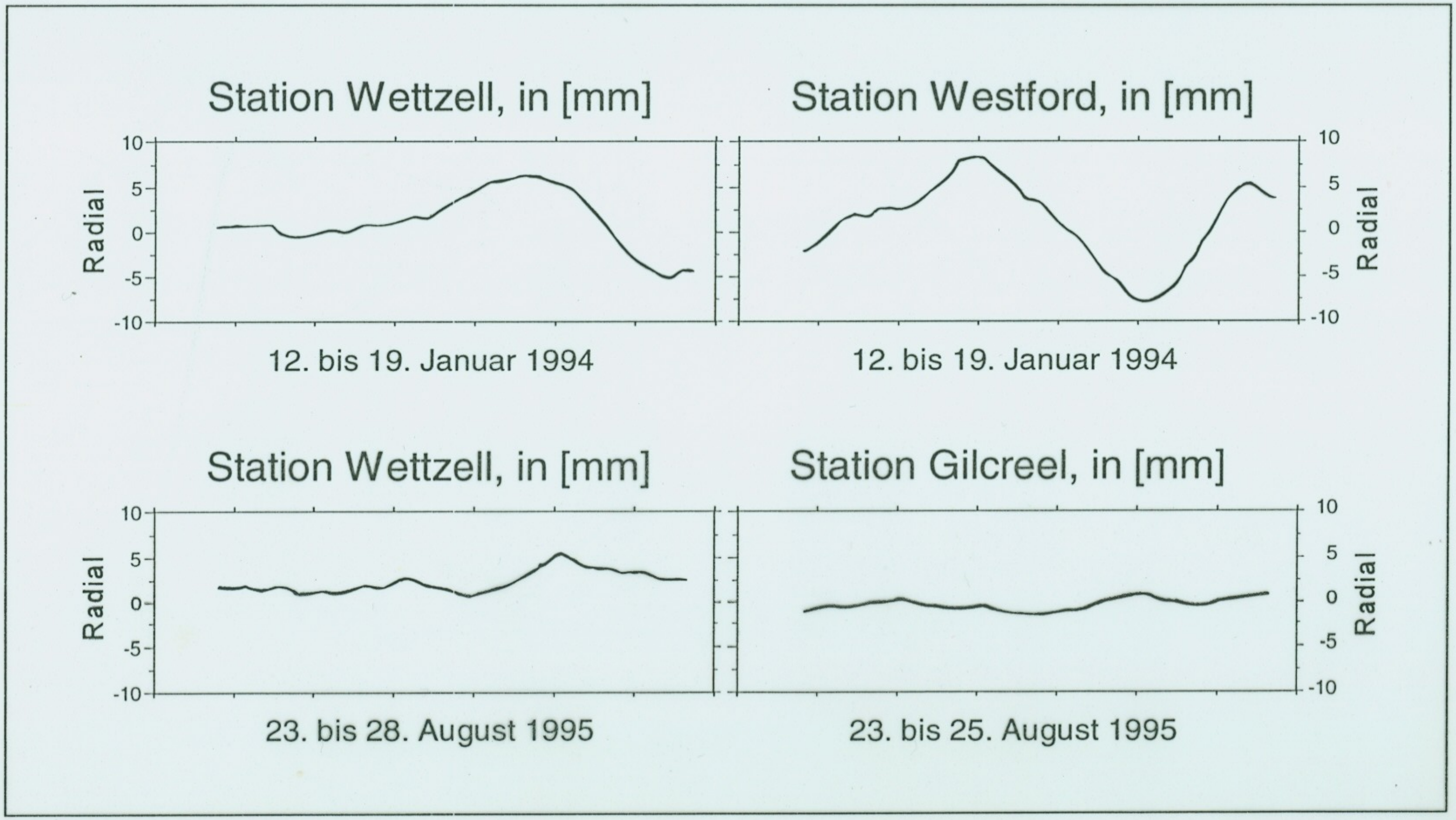




DGFI

**3.4 Analysis:**

# Clock drift 98APR20

**left:** residuals without including a clock drift
**right:** clock function

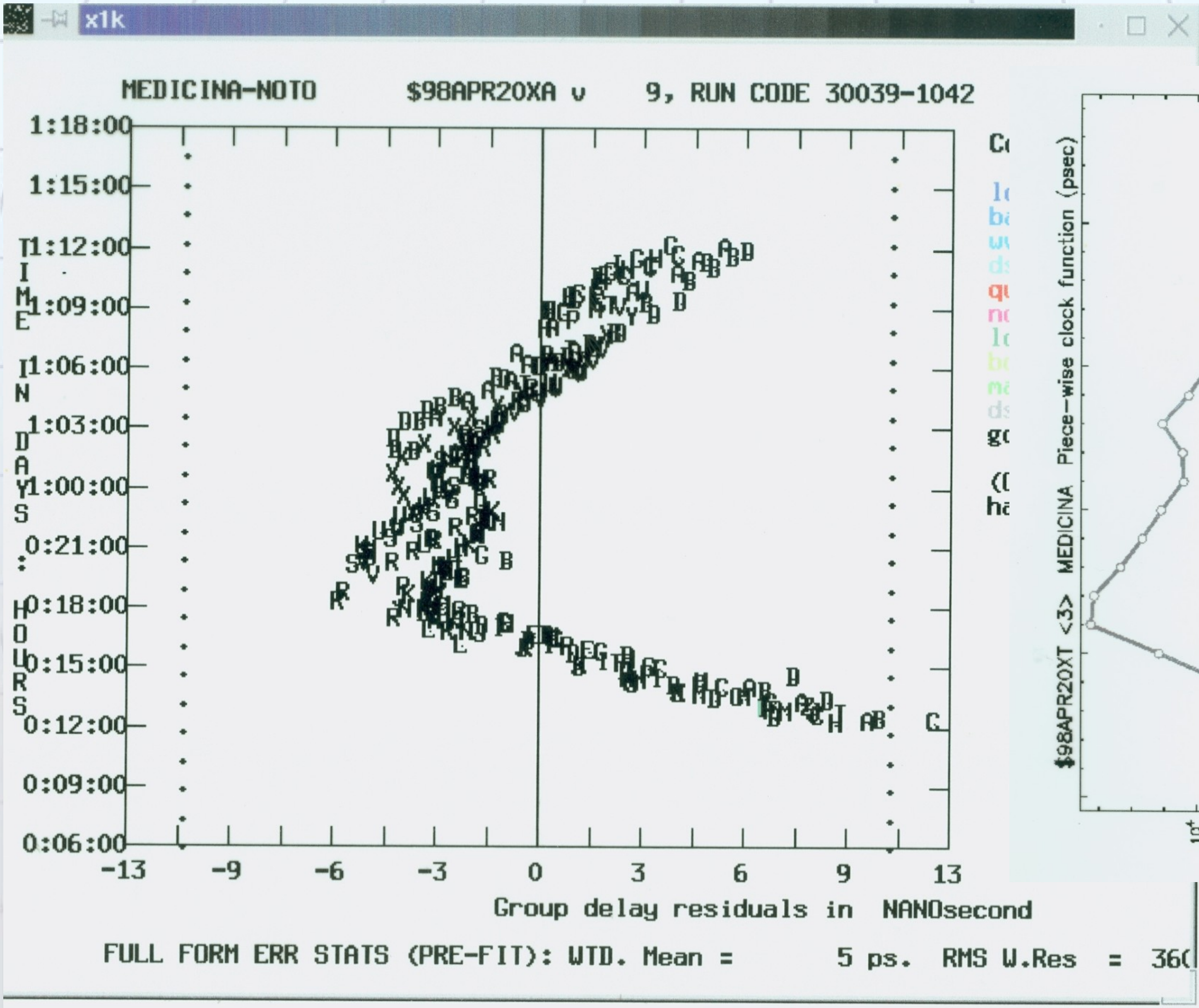


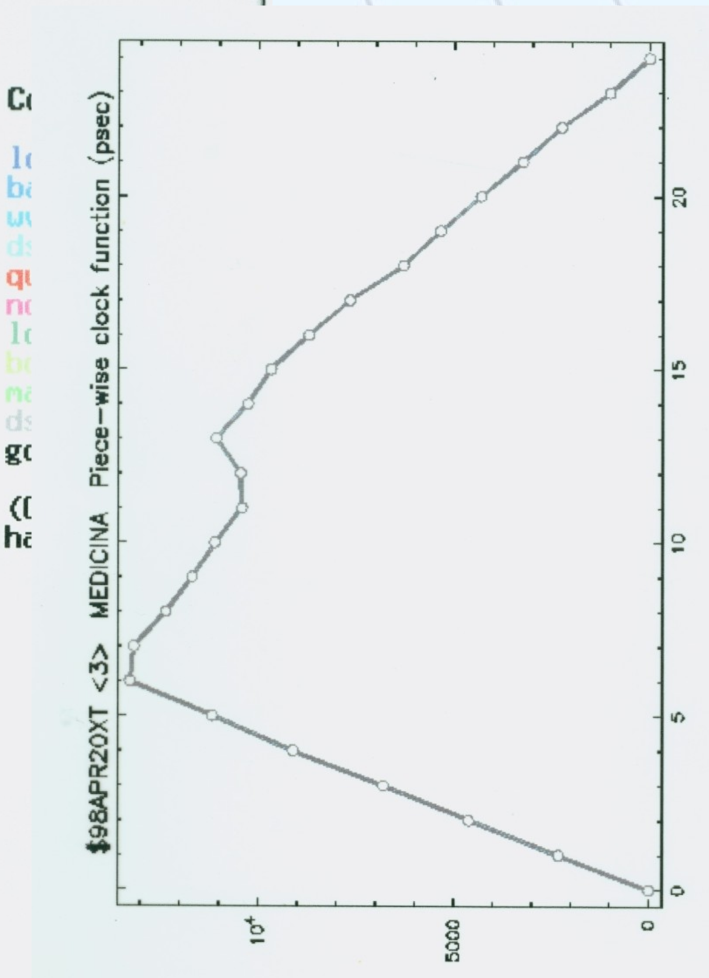

**3.4 Analysis:**

# Clock drift

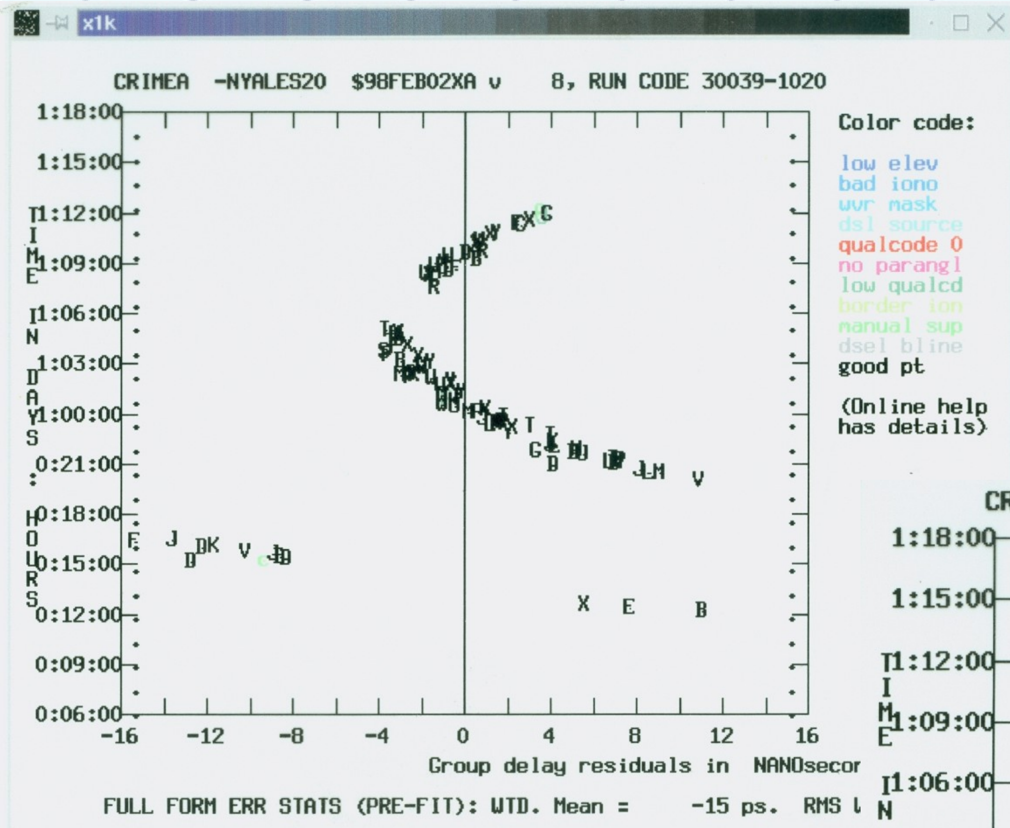


Clock not modelled
10 ns = 3 m

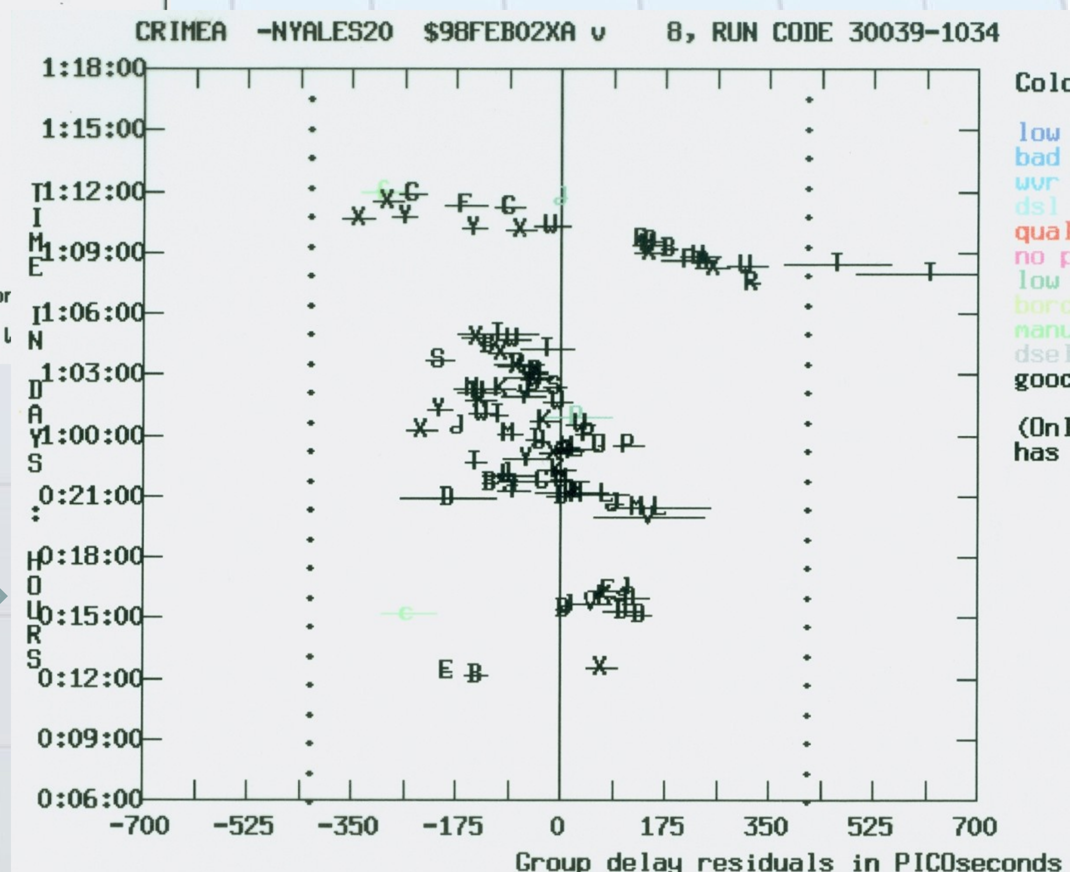


Clock modelled
100 ps = 3 cm

## 3.4.1 Theoretical delay:

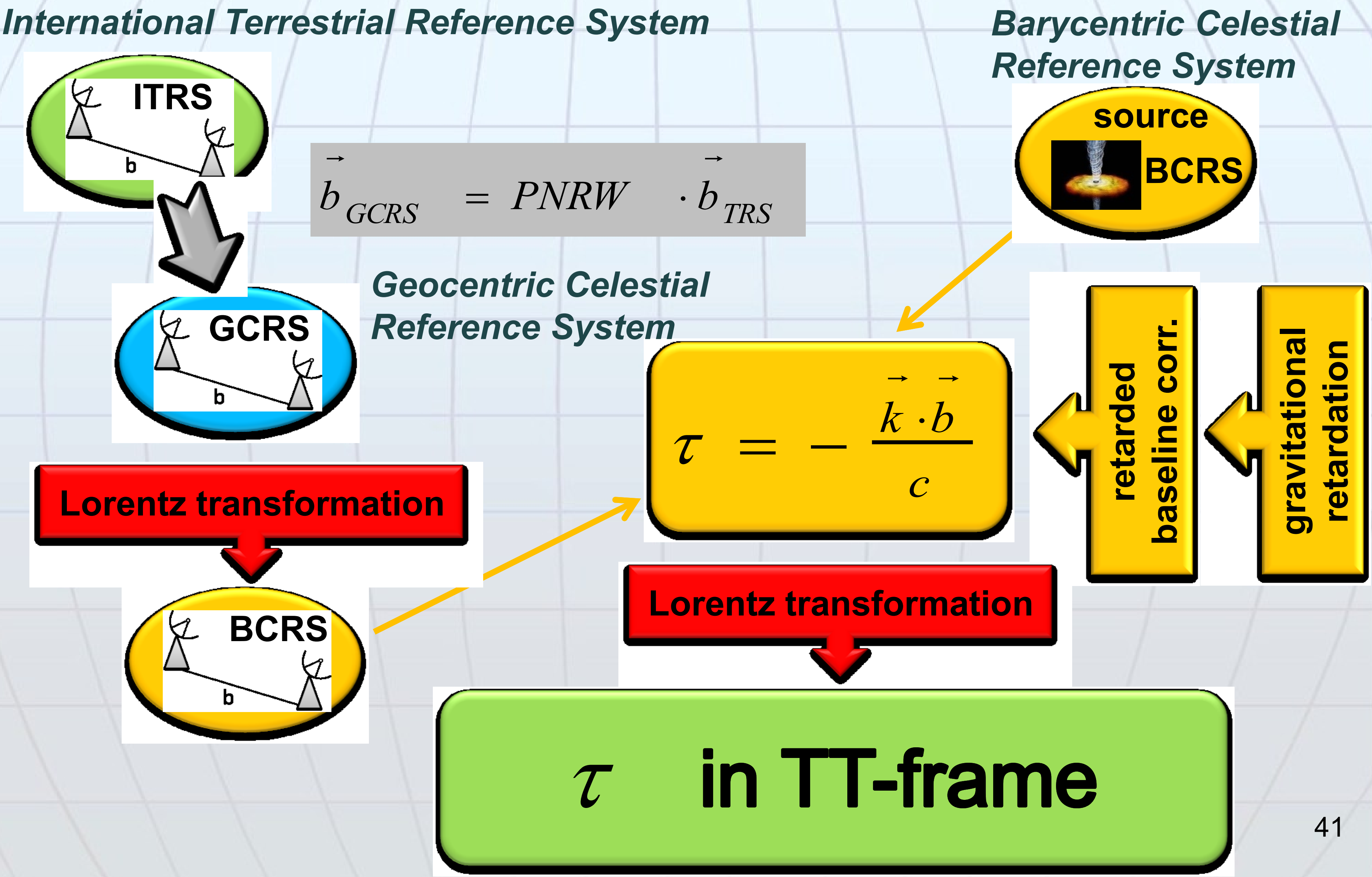

## 3.4.1 Theoretical delay:

**Delay in BRS:**

$$\tau_{BRS} = \frac{\vec{k} \cdot \vec{b}_{BRS}}{1 - \vec{k} \cdot v_2}$$

Movement of station 2, *retarded baseline correction*

**Differential gravitational delay:**

$$\Delta T_{grav} = \sum_j 2 \frac{GM_j}{c^3} ln \frac{|\vec{R}_{1j}| + \vec{k} \cdot \vec{R}_{1j}}{|\vec{R}_{2j}| + \vec{k} \cdot \vec{R}_{2j}}$$

*1,2 ….. station*
*j ….. disturbing body (Sun, Moon, Planets)*

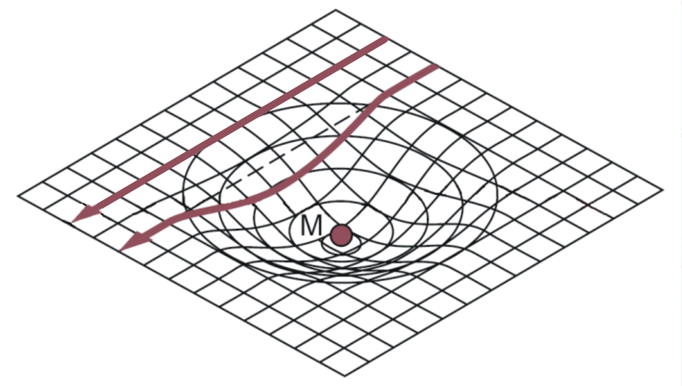


**Geocentric delay, '*Consensus*' *model*:**

$$\tau_{geo} = \frac{\Delta T_{grav} - \frac{\vec{K} \cdot \vec{b}}{c} \left[1 - \frac{(1+\gamma)U}{c^2} - \frac{v_{earth}^2}{2c^2} - \frac{v_{earth} \cdot v_{station2}}{c^2}\right] - \frac{\vec{v}_{earth} \cdot \vec{b}}{c^2}(1 + \vec{K} \cdot \vec{v}_{earth}/2c)}{1 + \frac{\vec{K}(\vec{v}_{earth} + \vec{v}_{station2})}{c}}$$

**Source vector:**

$$\vec{K} = \begin{pmatrix} -cos\alpha \cdot cos\delta \\ -sin\alpha \cdot cos\delta \\ -sin\delta \end{pmatrix}$$

## 3.4.1 Theoretical delay:

### 3. Der relativistische Gravitationseinfluß auf die VLBI - Beobachtungen

$$\tau^s_{grav} = (r^s_g/c)\cdot \ln\left[(|\vec{R}^s_1| + \vec{R}^s_1\cdot\vec{k})\ /\ (|\vec{R}^s_2| + \vec{R}^s_2\cdot\vec{k})\right]$$

$r^s_g$ – Schwarzschild-Radius der Sonne

$$r^s_g = (1+\gamma)\cdot G\cdot M^s/c^2$$

mit $M^s$ – Masse der Sonne, G – Gravitationskonstante: $r^s_g \approx 3\,\text{km}$

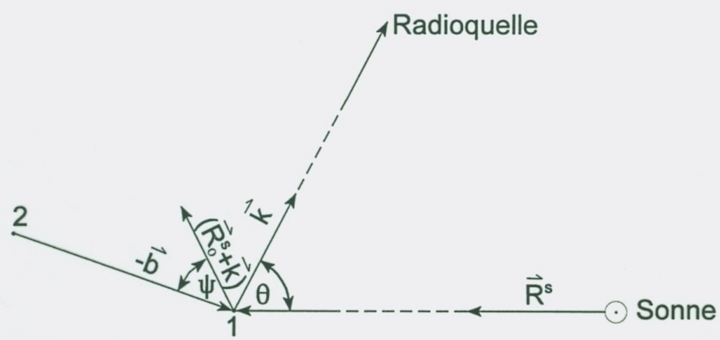


$$\tau^s_{grav} = (r^s_g/c)\cdot b\cdot\cos(\psi)/(|\vec{R}^s|\sin(\Theta/2))$$

$\tau^s_{grav}$ ist
- proportional zur Basislänge $b$
- umgekehrt proportional zu $\sin(\Theta/2)$
- umgekehrt proportional zur Entfernung zur Sonne $|\vec{R}^s|$
- abhängig von $\psi$

DGFI

### Maximale Laufzeitkorrekturen $\tau^s_{grav}$ wegen des relativistischen Gravitationseinflusses der Sonne

| $\Theta$ [°] | $\tau^s_{grav}$ [nsec] |
|---|---|
| 0,267 | 169,52 |
| 1 | 45,30 |
| 5 | 9,06 |
| 10 | 4,54 |
| 30 | 1,53 |
| 60 | 0,79 |
| 90 | 0,56 |
| 120 | 0,46 |
| 150 | 0,41 |
| 180 | 0,40 |

mit $\Theta$ – ∢ Radioquelle, Sonnenzentrum und b = 6000 km

DGFI

## 3.4.1 Theoretical delay:

**Beispiel für den relativistischen Gravitationseinfluß der Sonne**

(Experiment HAYSTACK – EFFELSBERG, 5/6 Mai, 1983)

$\tau$-Residuen ohne Berücksichtigung von $\tau^{s}_{grav}$ ($\sigma_{\tau} = 0{,}32$ nsec)

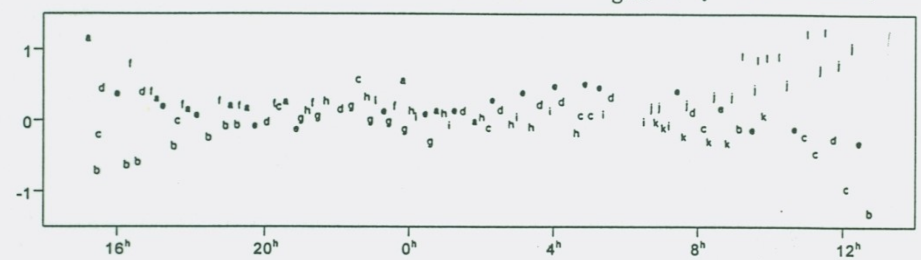


| | | | |
|---|---|---|---|
| a: | 4039.25 | g: | 3C273B |
| b: | 0528+134 | h: | OQ208 |
| c: | 0522+398 | i : | 3C345 |
| d: | 0212+735 | j : | 3C454.3 |
| e: | 180+784 | k: | 2216-038 |
| f: | 0J287 | l : | 0106-013 |

Korrekturen $\tau^{s}_{grav}$

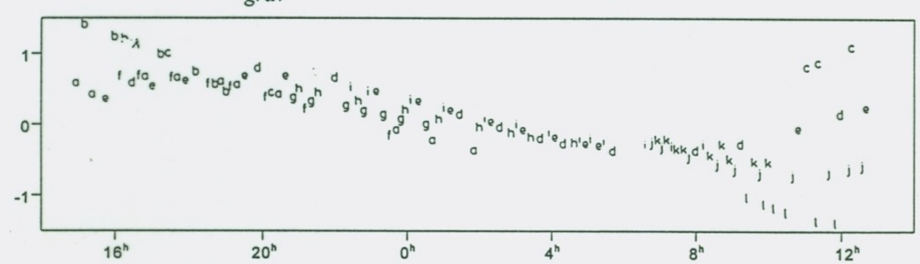


$\tau$-Residuen nach Berücksichtigung von $\tau^{s}_{grav}$ ($\sigma_{\tau} = 0{,}12$ nsec)


DGFI

## 3.4.2 Adjustment:

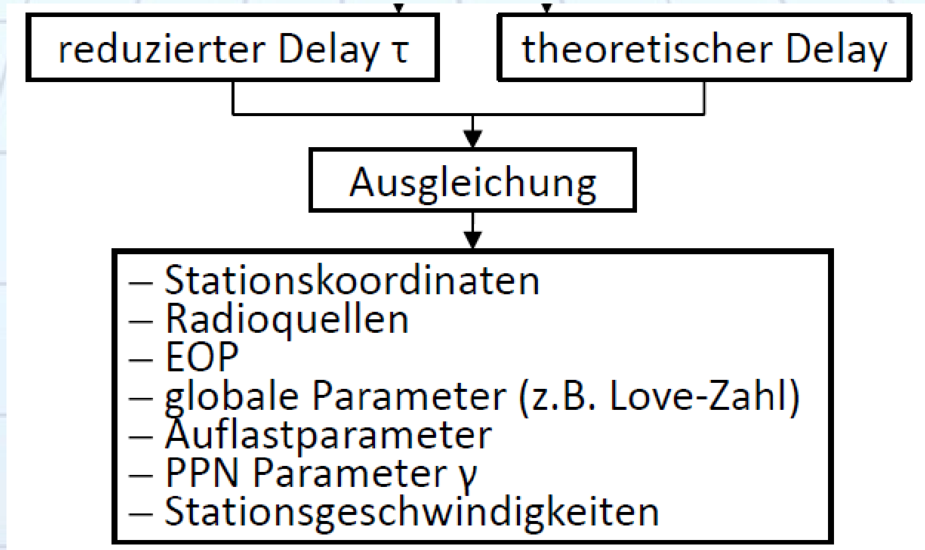


The design matrix includes the partial derivatives of the parameters of interest w.r.t. the observable:

$$\frac{\partial \tau}{\partial VAR} = \frac{1}{c} \cdot \frac{\partial(\vec{k} \cdot \vec{b})}{\partial VAR}$$

# IVS Products

- Earth Orientation Parameters (EOP):
  - 24-hour sessions (all EOP)
  - 1-hour Intensives (UT1−UTC)
- Terrestrial Reference Frame (TRF)
  - VLBI Terrestrial Reference Frame (VTRF)
- Celestial Reference Frame (CRF)
- Daily EOP+station coordinates (SINEX-files)
- Tropospheric Parameters (TROPO)
- Baseline Lengths (BL)

# Combined EOP are regular IVS products

Analysis Coordinator: Axel Nothnagel, Univ. Bonn,Germany

**Combined solution; every combination is more accurate than a single solution (robustness, reliability)**

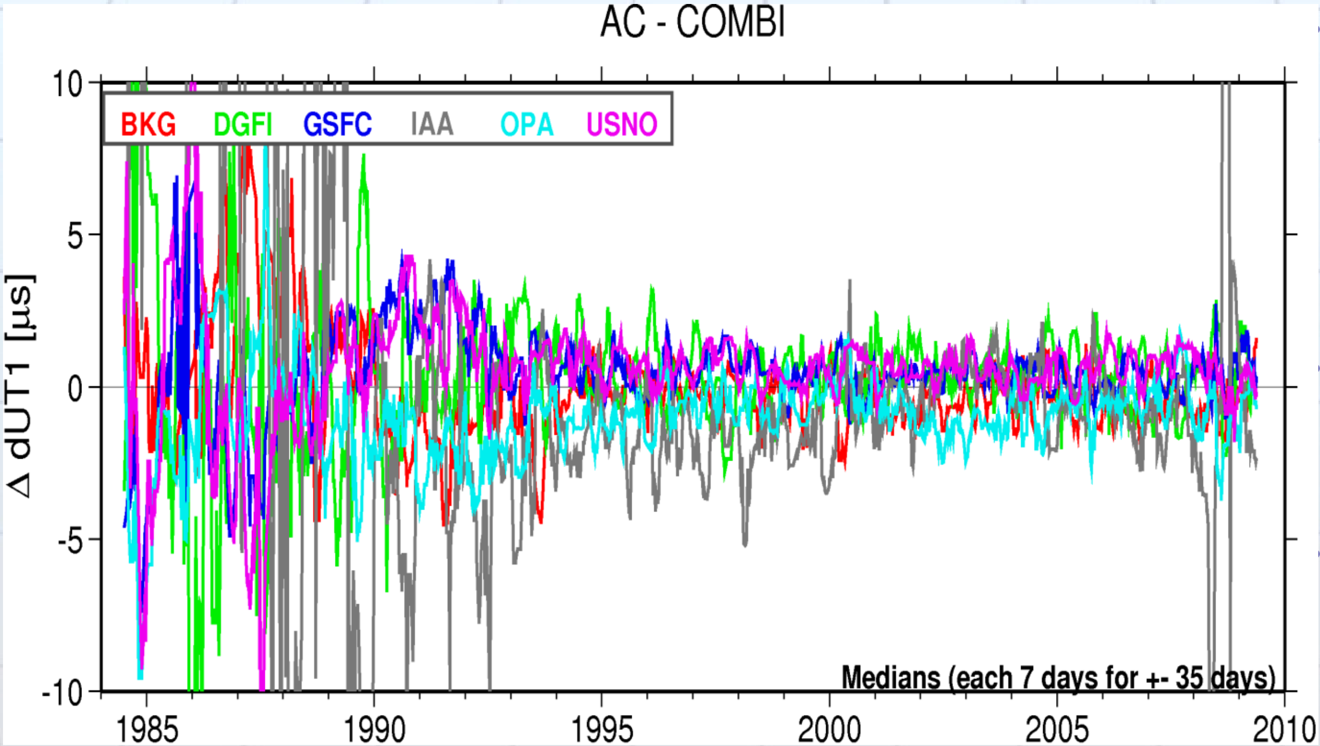


UT1-UTC residuals
*[A. Nothnagel, IVS Analysis Coordinator, 2011 http://vlbi.geod.uni-bonn.de/IVS-AC]*

- **Complete set of EOP**
  - $d\psi$, $d\varepsilon$
  - $x_p$ ,$y_p$
  - UT1-UTC
- **Combined solution from 6 Analysis Centers**
- **20-30% improvement**
  - accuracy
  - robustness
- **R1 & R4 since 2002**

# VLBI product: EOP

- Earth rotation parameters $x_{pole}$, $y_{pole}$, dUT1
- Precession / Nutation parameters
  nutation period: 18.6 y

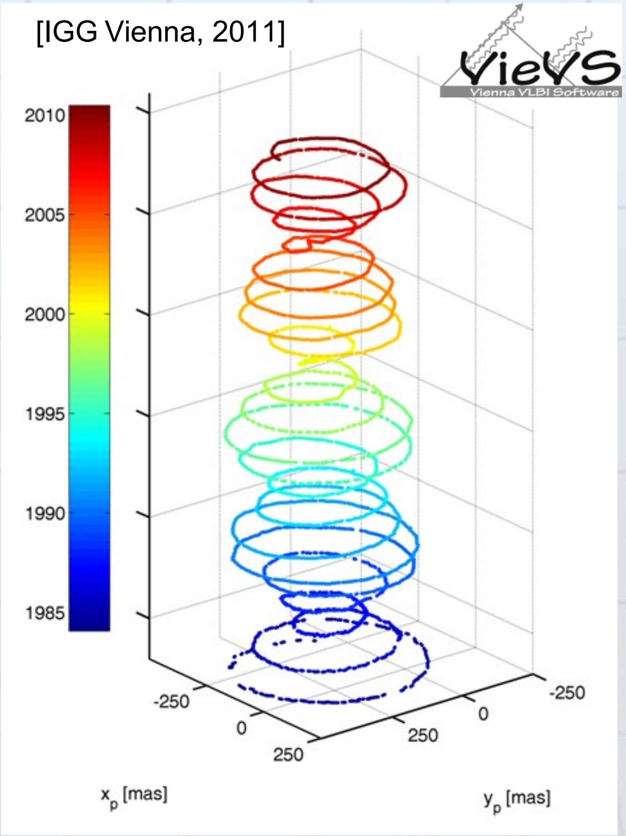


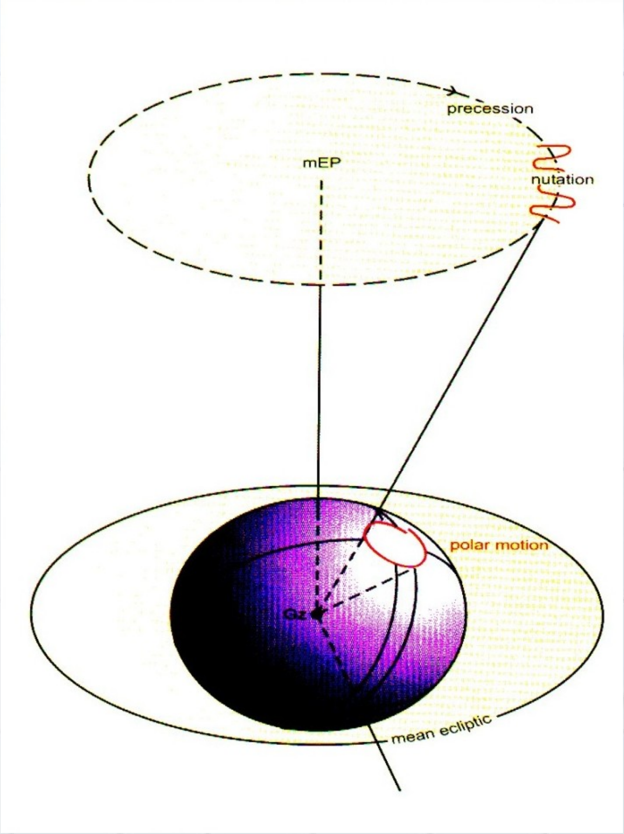

# VLBI product: Station velocities

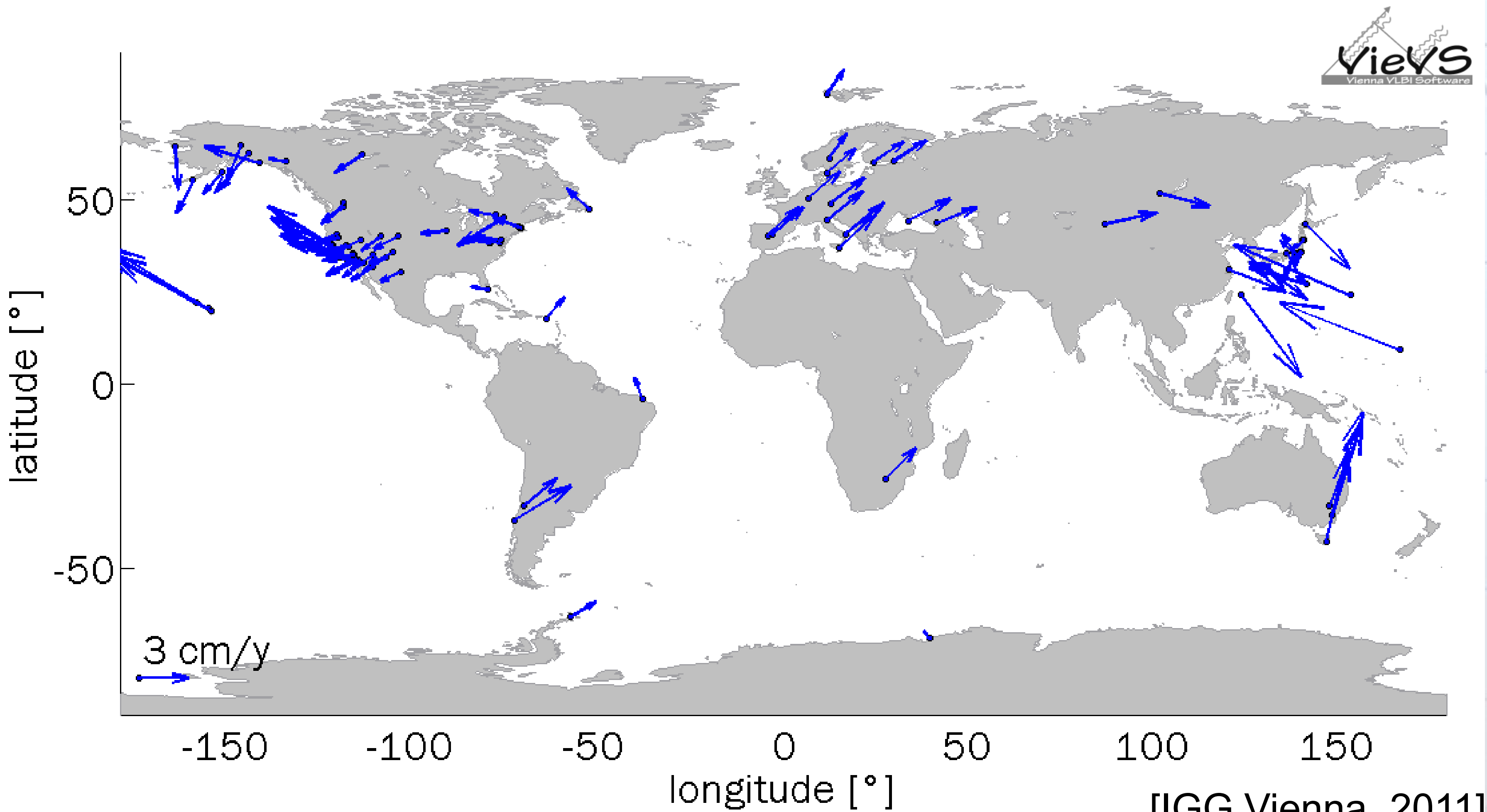


[IGG Vienna, 2011]

IVS Pilot Project: **Time Series of Baseline Lengths**

Plate motion: 2 stations per plate → transformation verctor + rotation
→ convert to horizontal movement

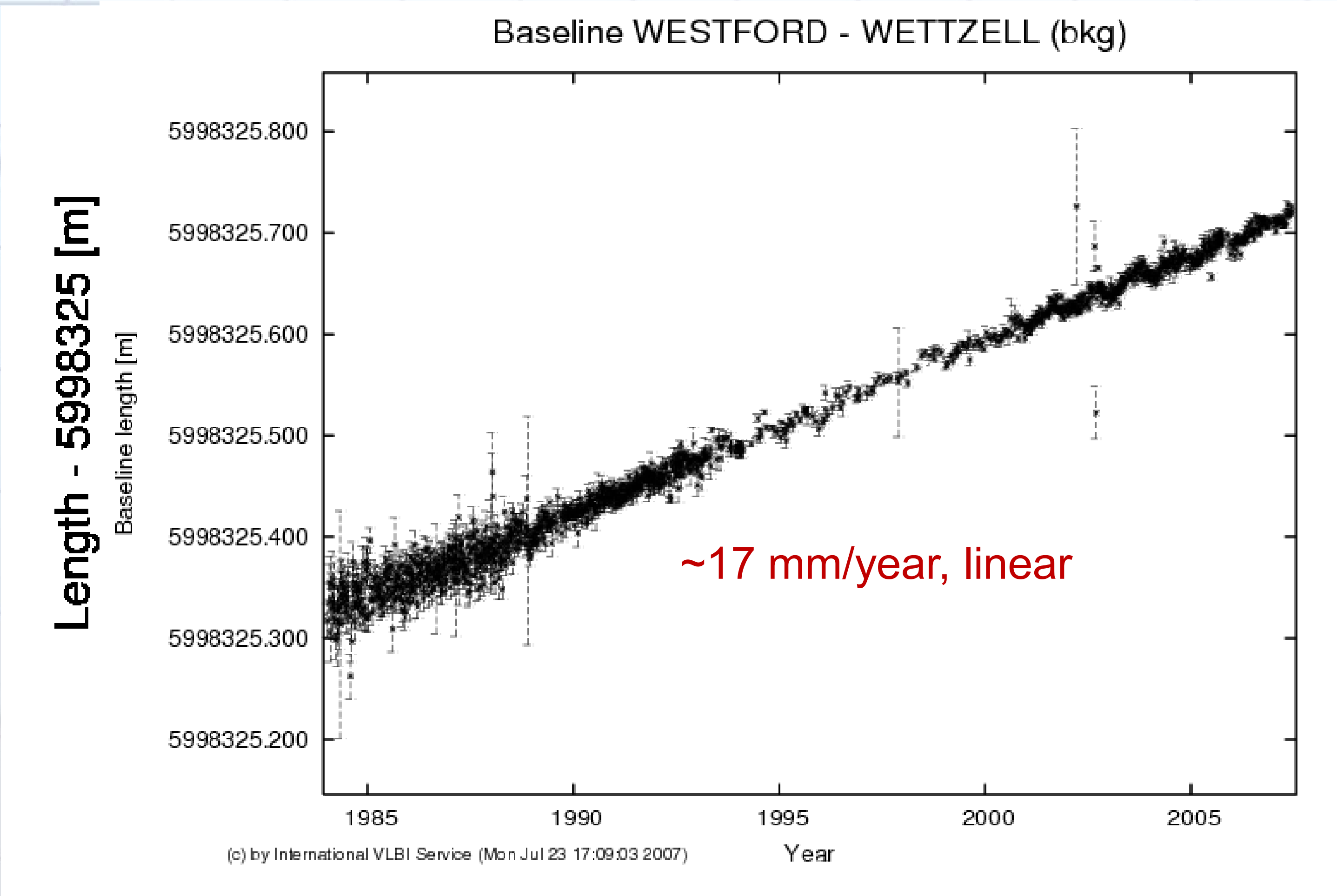


shown: evolution of the distance between the stations Westford (US) and Wettzell (EUR); ~ 6000 km
Observe the increase of accuracy!

# Displacement of TIGO Concepción

- The Earthquake moved Concepción by about 3 m to the west

- Similar results are obtained from GPS measurements

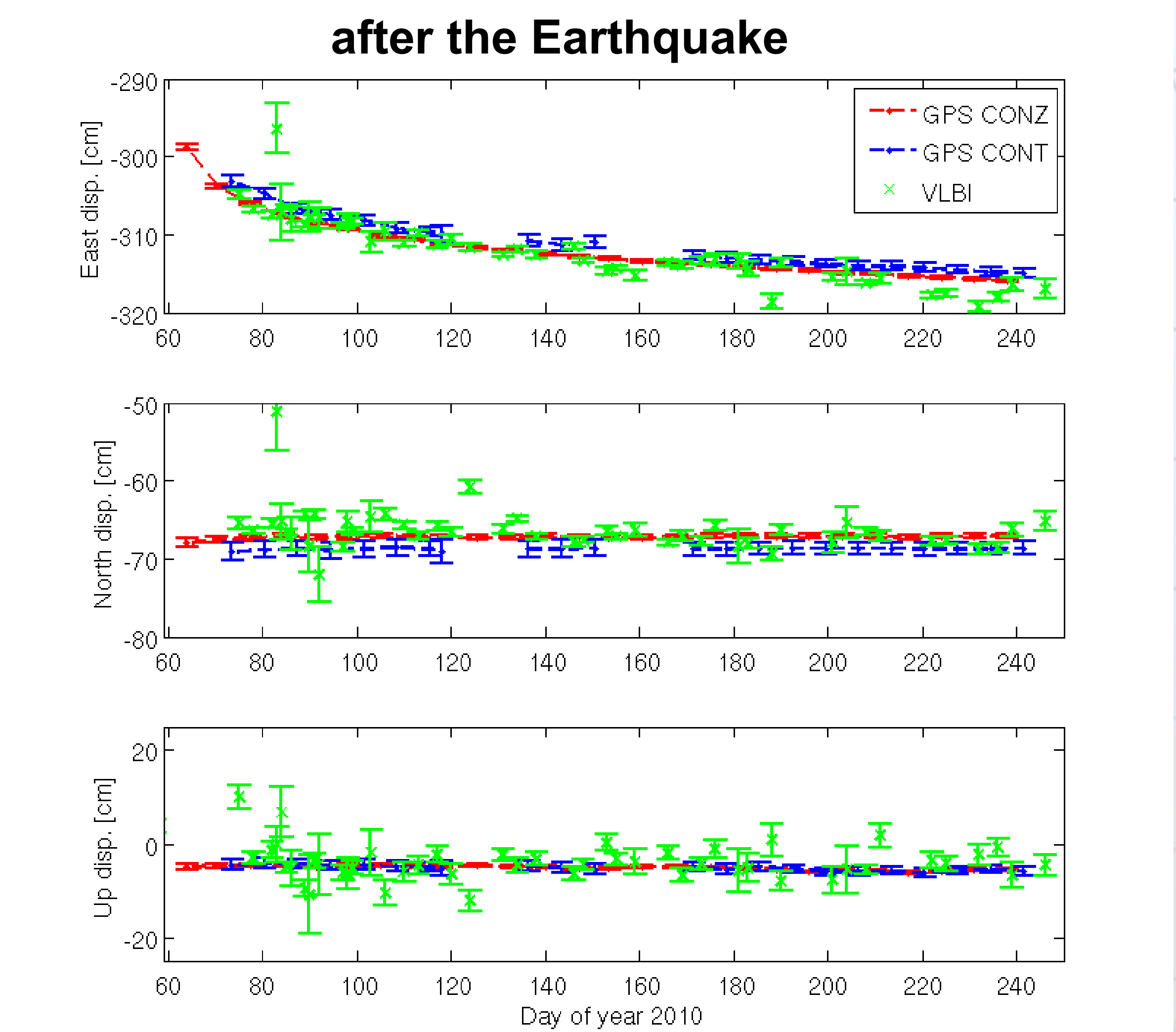


[IGG Vienna, 2010]

# VLBI product: Station motions

- Displacement of the TIGO radio telescope in Concepción caused by the magnitude 8.8 Earthquake on Feb 27, 2010.

# Climate studies using VLBI

- Long time-series of Zenith Wet Delays (ZWD) can be used for climate studies
- To detect climate change series with high stability are needed

see also: R. Heinkelmann, 2008

[Schuh et al., 2006]

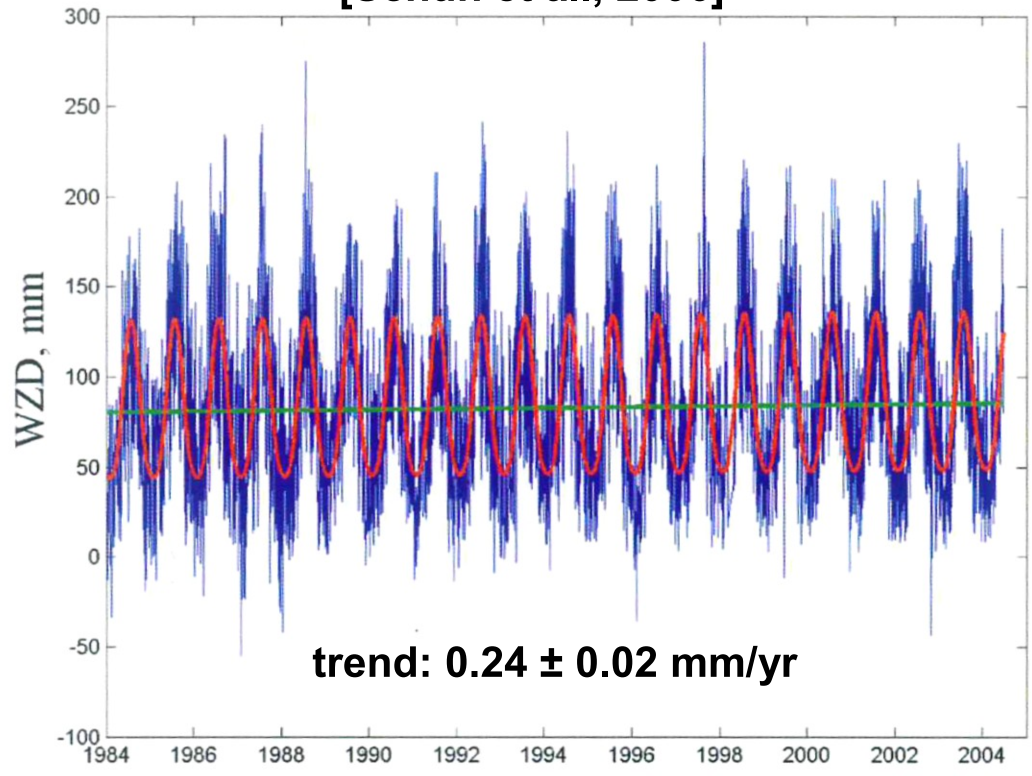


Wet zenith delays (blue) at Wettzell from VLBI obtained at IGG, annual and semiannual signal (red), linear trend (green).

# IVS Products

## Relativistic PPN parameter γ

| | | |
|---|---|---|
| $\gamma$ | „Mass-induced spatial curvature“<br>Light deflection | ≡ 1 (GR-Einstein) |

- **Gravitational delay of mass n**

$$\tau_{g,n} = (1+\gamma)\cdot\frac{GM_n}{c^3}\cdot\ln\left(\frac{\left|\vec{\mathbf{x}}_{1,n}\right| + \vec{\mathbf{x}}_{1,n}\cdot\vec{\mathbf{k}}}{\left|\vec{\mathbf{x}}_{2,n}\right| + \vec{\mathbf{x}}_{2,n}\cdot\vec{\mathbf{k}}}\right)$$

- **Higher order effect, relevant for small angular distances**

$$\tau_{ppn,n} = (1+\gamma)^2\cdot\frac{(GM_n)^2}{c^5}\cdot\frac{\vec{\mathbf{b}}\circ\left(\frac{\vec{\mathbf{x}}_{1,n}}{\left|\vec{\mathbf{x}}_{1,n}\right|} + \vec{\mathbf{k}}\right)}{\left(\left|\vec{\mathbf{x}}_{1,n}\right| + \vec{\mathbf{x}}_{1,n}\cdot\vec{\mathbf{k}}\right)^2}$$

# Relativistic PPN parameter γ from VLBI

## → Confirmation of Einstein’s theory

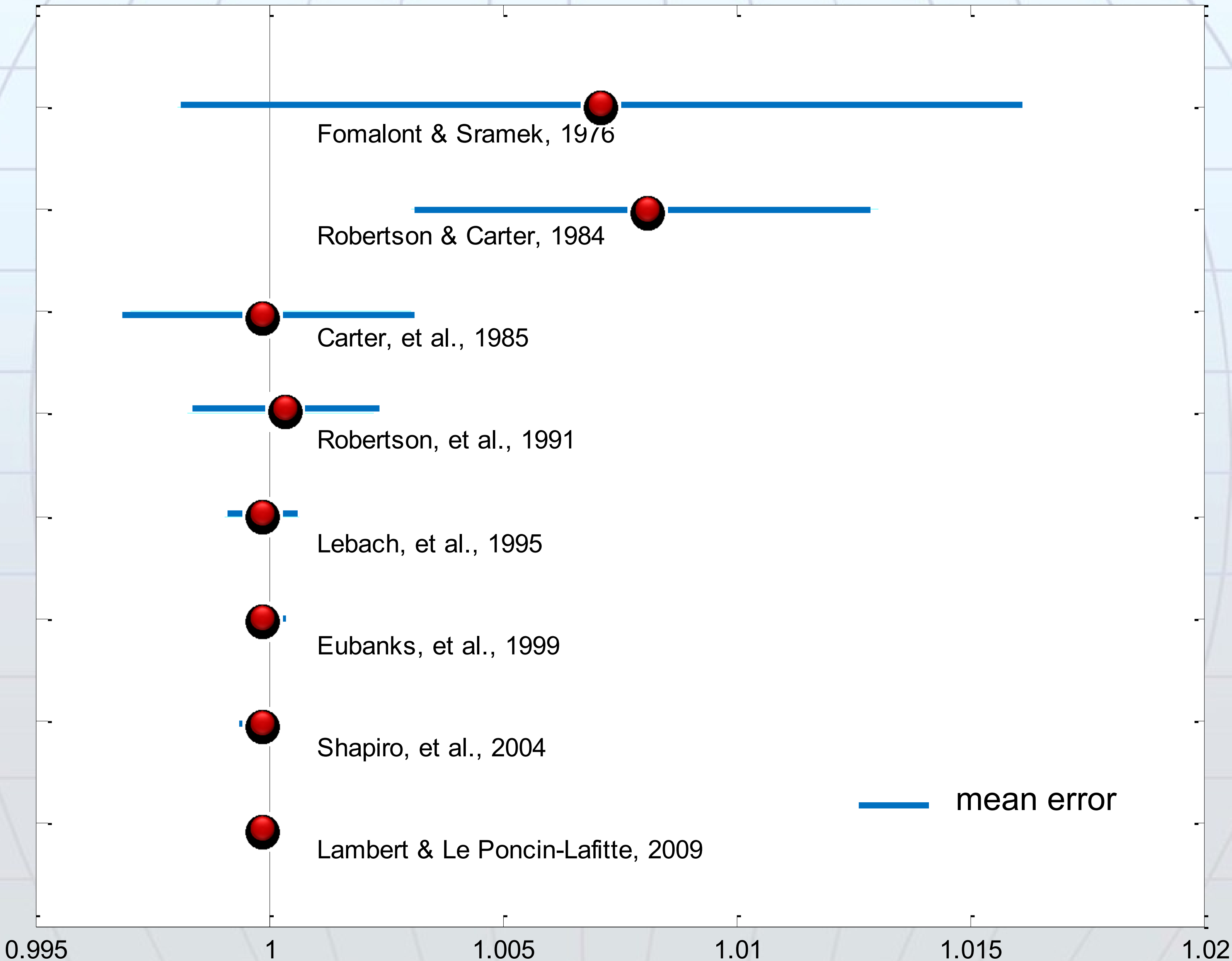

# The IVS delivers unique parameters…

[M. Rothacher]

| Parameter Type | VLBI | GNSS | DORIS | SLR | LLR | Altimetry |
|---|---|---|---|---|---|---|
| ICRF (Quasars) | **X** | | | | | |
| Nutation, Precession | **X** | (X) | | (X) | X | |
| Polar Motion | X | X | X | X | X | |
| UT1 | **X** | | | | | |
| Length of Day | (X) | X | X | X | X | |
| ITRF (Stations) | X | X | X | X | X | (X) |
| Geocenter | | X | X | X | | X |
| Gravity Field | | X | X | X | (X) | X |
| Orbits | | X | X | X | X | X |
| LEO Orbits | | X | X | X | | X |
| Ionosphere | X | X | X | | | X |
| Troposphere | X | X | X | | | X |
| Time Freq./Clocks | (X) | X | | (X) | | |

# VLBI for space applications

- **Satellite VLBI**
  - Tracking of GNSS satellites (e.g. Tornatore et al., 2010)
  - e.g. Geodetic Reference Antenna in Space (GRASP) (Y. Bar-Sever)
  - e.g. Microsatellites for GNSS Earth Monitoring (MicroGEM)
- **Differential VLBI (D-VLBI)**
  - Quasar – space craft (SC)
    - Deep space navigation
    - DSN, ΔDOR
    - NASA, ESA
  - SC – SC
    - multi-frequency method
    - same beam method
    - e.g. SELENE (JAXA)

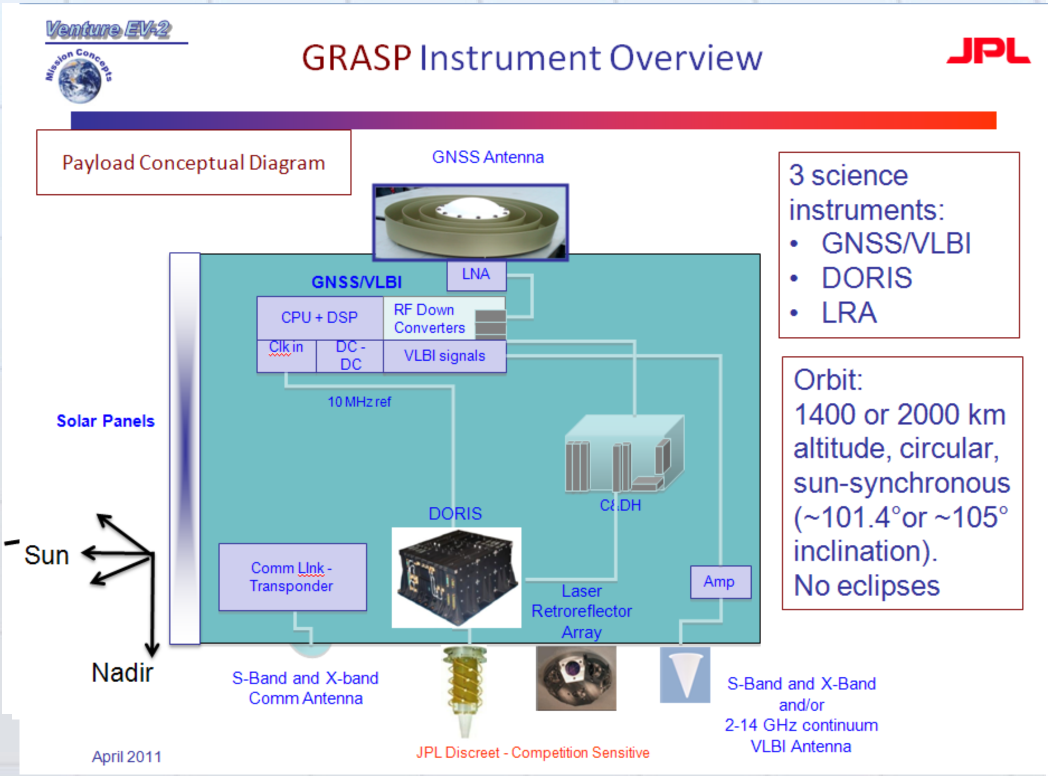

# Importance of VLBI for Geodesy and Astronomy

- VLBI is crucial for the

- realization of the international terrestrial reference frame (**ITRF**) – particularly for the scale
- measurement of **polar motion** and lots of other geodynamic/astronomic parameters (Love and Shida numbers, loading coefficients, relativistic parameter $\gamma$...)

# Importance of VLBI for Geodesy and Astronomy

- VLBI is **essential** for the
  - measurement of **UT1** and of **Nutation**/Precession

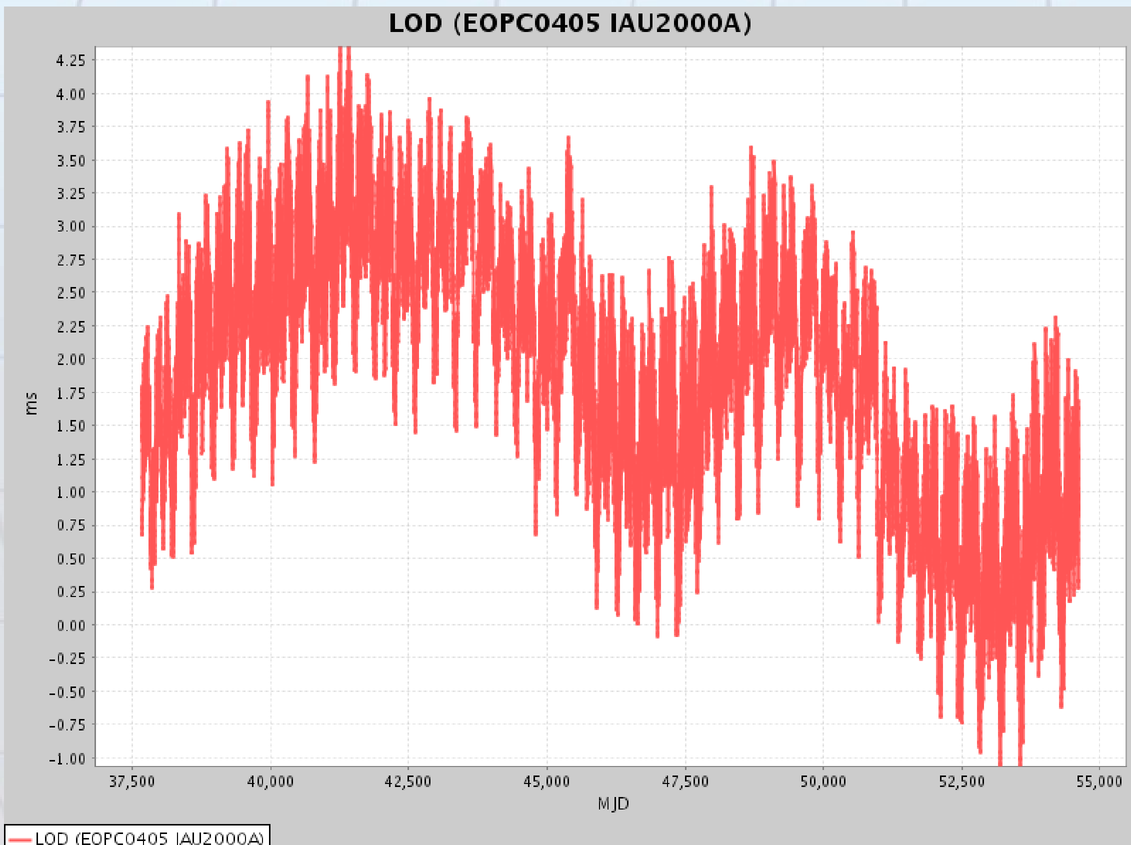


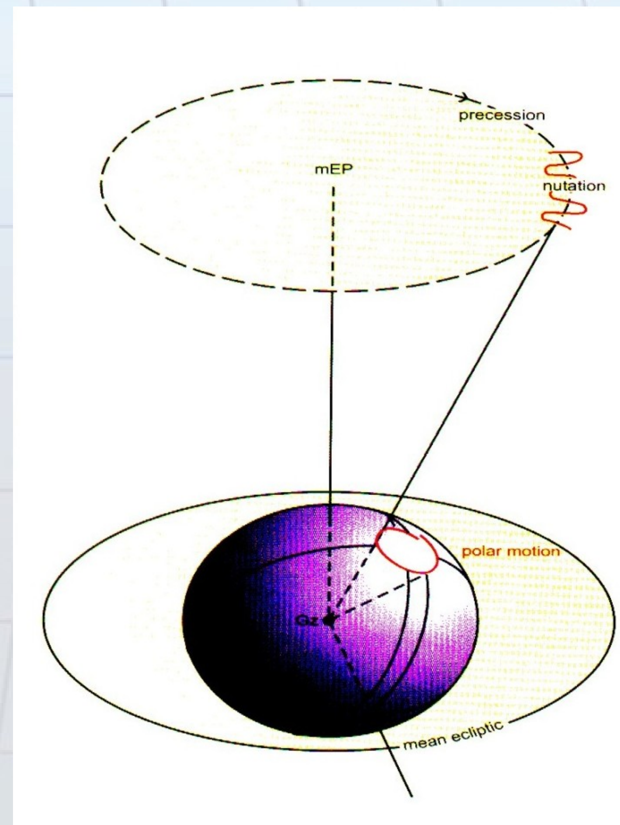

# Importance of VLBI for Geodesy and Astronomy

- VLBI ist **essential** for the
  - measurement of **UT1** and of **Nutation**/Precession

  - **Realization of the celestial reference frame (ICRF) of extragalactic radio sources**